

Aus der Strahlenklinik  
der Friedrich-Alexander-Universität Erlangen-Nürnberg  
Direktor: Prof. Dr. R. Fietkau

---

**Evaluation of the prognostic significance of regulatory T  
cells und killer T cells in Glioblastoma**

Inauguraldissertation  
zur Erlangung der Doktorwürde  
der Medizinischen Fakultät  
der Friedrich-Alexander-Universität Erlangen-Nürnberg

vorgelegt von  
Afsal Sharafudeen  
aus  
Alleppey



**Als Dissertation genehmigt von der  
Medizinischen Fakultät der Friedrich-Alexander-Universität  
Erlangen-Nürnberg**

Dekan: Prof. Dr. Markus F. Neurath  
Referent: Prof. Dr. Luitpold Distel  
Korreferent: Prof. Dr. Rainer Fietkau  
Tag der mündlichen Prüfung: 28. März 2023

Für meine Eltern

1	Summary.....	6
	1.1 Background .....	6
	1.2 Methods.....	7
	1.3 Results and Conclusion.....	7
2	Zusammenfassung.....	8
	2.1 Hintergrund .....	8
	2.2 Methoden.....	9
	2.3 Ergebnisse und Schlussfolgerung .....	10
3	Introduction.....	11
	3.1 Glioblastoma .....	11
	3.1.1 Epidemiology .....	11
	3.1.2 Biology and Histology .....	12
	3.1.3 Localization and clinical presentation.....	13
	3.1.4 Imaging and Diagnosis.....	14
	3.1.5 Molecular markers.....	16
	3.1.6 Therapy.....	16
	3.1.7 Other therapeutic Approaches .....	18
	3.1.8 Prognosis and factors affecting prognosis .....	20
	3.2 Immune system.....	20
	3.2.1 Immune system vs cancer .....	21
4	Abstract.....	24
5	Method.....	25
	5.1 Studied glioblastoma cohort.....	25
	5.2 Production of the tissue microarrays (TMA) .....	25
	5.3 Immunohistochemical staining.....	27
	5.4 Analysis.....	28
	5.4.1 Cell counts and cell density.....	29
	5.4.2 Statistics.....	29
6	Results .....	30
	6.1 Immune cell density.....	30
	6.1.1 Density of CD8+ Lymphocytes in the 5 ROI .....	30
	6.1.2 Density of FoxP3+ Lymphocytes in the 5 ROI .....	31
	6.1.3 Comparison of mean cell density-es of CD8+ an d FoxP3+ Lymphocytes .....	32
	6.1.4 Correlation between cell density and survival.....	33
7	Discussion.....	53
	7.1 Method.....	53
	7.2 Results.....	54

7.3	TILs as prognostic factors in Glioblastoma .....	54
7.3.1	CD8+ cytotoxic T cells as a prognostic factor? .....	54
7.3.2	FoxP3+ regulatory T cells as a prognostic factor? .....	56
8	Bibliography .....	57
9	Abbreviations .....	66
10	Illustrations .....	68
11	Acknowledgement.....	71

# 1 Summary

## 1.1 Background

For more than 15 years there has been no significant increase in the survival span among Glioblastoma (GBM) patients, despite the intensive research on this most aggressive and most common glial tumor (Bleeker et al., 2012). As such the treatment for this cancer is in desperate need of progress. In our study we examined the predictive and prognostic significance of two important immune cells in its tumor microenvironment (TME) among a retrospective patient collective, where they underwent surgery or radiochemotherapy (RCT) or both. The progression free survival (PFS) and overall survival (OS) were set as endpoints.

In 2013 a norwegian study on 65 GBM patients could prove that the Infiltration of CD8+ (Cluster of differentiation 8+) and CD3+ tumor infiltrating Lymphocytes (TILs) was associated with prolonged survival (Kmiecik et al., 2013). Yet the following year, the same results could not be reproduced in a group of 90 patients (Han et al., 2014). But they also found that a higher density of CD4+ with a lower density of CD8+ in the tumor was associated with a significantly bad prognosis. A further study on 62 patients identified the prognostic significance of regulatory FoxP3+ (forkhead box protein 3+) TIL, it was found that these cells negatively influence the progression free and overall survival (Yue et al., 2014). But a study by Thomas et al. (2015) on a smaller Patient population (n=25) questioned this result. A further Research from Vienna (Berghoff et al., 2015) couldn't find any prognostic significance for CD3+, CD8+, PD1+ and CD20+ TILs among 117 GBM patients. Furthermore a correlation between the density of different TILs in the TME and its progress or survival rate has already been proven for many non-central nervous system cancers such as head and neck squamous cell carcinoma (Echarti et al., 2019), Hodgkin lymphoma (Álvaro et al., 2005), ovarian carcinoma (Santoiemma & Powell, 2015), breast cancer (Salgado et al., 2015) etc.

## **1.2 Methods**

Tissue Microarrays (TMA) were created from the tissue samples of 104 GBM patients. Then a double staining method was implemented to mark 2 kinds of TILs. In this method antibodies against the forkhead box protein P3 (FoxP3) were used to identify regulatory T lymphocytes (Tregs) and antibodies against CD8 were used to identify cytotoxic lymphocytes.

The Arrays were then digitalized and evaluated using the Biomas image analysis program (Prof. Dr. Distel, Department of Radiotherapy, University of Erlangen, Germany). The number of Tregs and cytotoxic T lymphocytes per square millimeter were thus determined in 5 different regions of interest (ROI): tumor core, necrosis, infiltration zone, peripheral zone and normal tissue surrounding tumor. For each ROI, two patient groups were created from the cohort by dividing them at the median cell density. Kaplan-Meier plots for overall survival and progression-free survival were made for both groups, and the difference between the two survival curves was analyzed for significance using the log-rank test of the SPSS analysis software. (IBM Deutschland GmbH, Nuremberg, Germany).

## **1.3 Results and Conclusion**

The density of CD8+ TIL in the tumor core was found to be of prognostic significance. The patients with a lower cell density of CD8+ cells in the tumor core than the median seem to have a better overall survival ( $p=0.028$ ). Other than this densities of the subgroups of TILs examined here (CD8+ cytotoxic T lymphocytes and FoxP3+ regulatory T lymphocytes) in the different ROI were not found to be of prognostic significance.

The distribution of the TILs didn't vary significantly among the four ROI containing tumor (tumor core, necrosis, infiltration zone and peripheral zone). However the normal brain tissue surrounding the tumor had significantly fewer of both these subgroup of TILs when compared with the other ROI.

This study further strengthens the assumption that interaction between GBM and our immune system tend to be heterogenous. Further similar research after patient stratification based on whether the tumor is primary or secondary in nature and if it is recurring as well as taking the immunohistochemical properties into account is required to determine whether a type of TIL or the ratio between different types of TILs in the TME can be of prognostic significance in any subgroups of GBM. This can in turn help develop and optimize TIL targeted immune therapy strategies in GBM.

## **2 Zusammenfassung**

### **2.1 Hintergrund**

Seit mehr als 15 Jahren hat sich die Überlebenszeit von Glioblastom-Patienten trotz intensiver Forschung über diesem aggressivsten und häufigsten glialen Tumor nicht wesentlich verlängert (Bleeker et al., 2012). Die Behandlung dieses Krebses braucht daher dringend Fortschritte. In unserer Studie untersuchten wir die prädiktive und prognostische Bedeutung von zwei wichtigen Immunzellen in der Tumormikroumgebung (TME) bei einem retrospektiven Patientenkollektiv, das sich einer Operation oder einer Radiochemotherapie (RCT) oder beidem unterzog. Als Endpunkte wurden das progressionsfreie Überleben und das Gesamtüberleben festgelegt.

Im Jahr 2013 konnte eine norwegische Studie an 65 GBM-Patienten nachweisen, dass die Infiltration von CD8<sup>+</sup> (Cluster of differentiation 8<sup>+</sup>) und CD3<sup>+</sup> tumorinfiltrierenden Lymphozyten (TILs) mit einem verlängerten Überleben verbunden war (Kmiecik et al., 2013). Im darauffolgenden Jahr konnten dieselben Ergebnisse in einer Gruppe von 90 Patienten jedoch nicht reproduziert werden (Han et al., 2014). Aber auch sie fanden heraus, dass eine höhere Dichte von CD4<sup>+</sup> kombiniert mit einer geringeren Dichte von CD8<sup>+</sup> im Tumor mit einer deutlich schlechteren Prognose verbunden war (Hazard Ratio 1,5 und 1,6). In



einer weiteren Studie an 62 Patienten wurde die prognostische Bedeutung von regulatorischen FoxP3+ (Forkhead Box Protein 3+) TIL ermittelt, und es wurde festgestellt, dass diese Zellen das progressionsfreie und das Gesamtüberleben negativ beeinflussen (Yue et al., 2014). Eine Studie von Thomas et al. (2015) an einer kleineren Patientenpopulation (n=25) stellte dieses Ergebnis jedoch in Frage. Eine weitere Untersuchung aus Wien (Berghoff et al., 2015) konnte bei 117 GBM-Patienten keine prognostische Bedeutung für CD3+, CD8+, PD1+ und CD20+ TILs feststellen. Darüber hinaus wurde eine Korrelation zwischen der Dichte verschiedener TILs im TME und dem Fortschreiten oder der Überlebensrate bereits für viele Krebsarten außerhalb des Zentralnervensystems nachgewiesen, z. B. für Plattenepithelkarzinome des Kopfes und Halses (Echarti et al., 2019), Hodgkin-Lymphome (Álvaro et al., 2005), Ovarialkarzinome (Santoiemma & Powell, 2015), Brustkrebs (Salgado et al., 2015) usw.

## **2.2 Methoden**

Aus den Gewebeproben von 104 GBM-Patienten wurden Tissue Microarrays (TMA) erstellt. Dann wurde eine Doppelfärbung angewandt, um 2 Arten von TILs zu markieren. Bei dieser Methode wurden Antikörper gegen das Forkhead-Box-Protein P3 (FoxP3) zur Identifizierung regulatorischer T-Lymphozyten (Tregs) und Antikörper gegen CD8 zur Identifizierung zytotoxischer Lymphozyten verwendet.

Die Arrays wurden anschließend digitalisiert und mit dem Bildanalyseprogramm Biomas (Prof. Dr. Distel, Klinik für Strahlentherapie, Universität Erlangen, Deutschland) ausgewertet. Auf diese Weise wurde die Anzahl der Tregs und zytotoxischen T-Lymphozyten pro Quadratmillimeter in 5 verschiedenen Regionen von Interesse (ROI) bestimmt: Tumorkern, Nekrose, Infiltrationszone, periphere Zone und den Tumor umgebendes Normalgewebe. Für jede ROI wurden aus der Kohorte zwei Patientengruppen gebildet, indem sie nach der mittleren Zelldichte geteilt wurden. Für beide Gruppen wurden Kaplan-Meier-Diagramme für das Gesamtüberleben und das progressionsfreie Überleben

erstellt, und der Unterschied zwischen den beiden Überlebenskurven wurde mit dem Log-Rank-Test der SPSS-Analysesoftware für Signifikanz analysiert (IBM Deutschland GmbH, Nürnberg, Deutschland).

### **2.3 Ergebnisse und Schlussfolgerung**

Es wurde festgestellt, dass die Dichte der CD8+ TILs im Tumorkern von prognostischer Bedeutung ist. Die Patienten mit einer geringeren Zelldichte von CD8+ Zellen im Tumorkern als dem Median scheinen ein besseres Gesamtüberleben zu haben ( $p=0,028$ ). Ansonsten waren die Dichten der hier untersuchten Untergruppen von TILs (CD8+ zytotoxische T-Lymphozyten und FoxP3+ regulatorische T-Lymphozyten) in den verschiedenen ROI nicht von prognostischer Bedeutung.

Die Verteilung der TILs variierte nicht signifikant zwischen den vier ROI mit Tumor (Tumorkern, Nekrose, Infiltrationszone und periphere Zone). Das normale Hirngewebe, das den Tumor umgibt, wies jedoch im Vergleich zu den anderen ROI deutlich weniger dieser beiden Untergruppen von TILs auf.

Diese Studie untermauert die Annahme, dass die Interaktion zwischen GBM und unserem Immunsystem tendenziell heterogen ist. Weitere ähnliche Forschung nach Stratifizierung von GBM Patienten, basierend darauf, ob sie primäres, sekundäres oder Rezidiv-GBM haben, und auch unter Berücksichtigung der immunhistochemischen Eigenschaften ist notwendig. So kann festgestellt werden, ob in diesen Untergruppen des GBMs eine Art von TIL oder das Verhältnis zwischen verschiedenen Arten von TILs in der TME von prognostischer Bedeutung sein kann. Die Ergebnisse können bei der Entwicklung und Optimierung von TIL-zielgerichteten Immuntherapiestrategien bei GBM helfen.

## **3 Introduction**

### **3.1 Glioblastoma**

GBM is the most aggressive of the primary brain tumors arising from the glial cells and unfortunately also the most common of them (Bleeker et al., 2012). Over the past few decades a lot of research has been done on GBM, which has led us to a finer understanding of the biological aspects of the tumor, but any relevant improvement in the overall survival of patients is yet to be achieved. Compared to the 1960s where a GBM patient had a survival rate of around 6 months from diagnosis (Oertel, von Buttlar, Schroeder, & Gaab, 2005), now it is still just 14,6 months with the actual standard therapy which was introduced in 2005 (Roger Stupp et al., 2005).

#### **3.1.1 Epidemiology**

GBM has an incidence of 2-4 per 100000 per year in industrialized countries (Wöhrer et al., 2009) The incidence of GBM in the white population is at least twice as high as in the black population and the incidence in developing countries seems to be lower (Ohgaki & Kleihues, 2005). Men are affected more frequently than women; GBM is much less common in children than in adults (Mahvash et al., 2011).

Usually there is no family history of cancers among GBM patients (Ranger et. al 2014). Exposure of the head and neck to ionizing radiation was found to be a risk factor and atopic diseases such as allergies, asthma, eczema and hay fever seem to have a protective effect against all brain tumors (Ostrom et al., 2019). In most of the patients it is diagnosed in the 6th or 7th decade of life (Dolecek et al 2012).

Most are primary GBMs (90%) and develop rapidly de novo in elderly patients. Secondary GBMs that manifest mostly in younger patients preferentially in frontal

lobe develop from lower Grade Gliomas and carry a significantly better prognosis (Ohgaki & Kleihues, 2013).

### **3.1.2 Biology and Histology**

Rudolf Virchow first described this tumor in 1863 and called it "spongioblastoma". The name Glioblastoma was coined later by Bailey and Cushing, due to its macroscopically colorful appearance, which is due to tumor necrosis and pathological hemorrhages (Kleihues and Cavenee, 2000). As shown in Figure 1, histologically this astrocytic tumor is characterized by a diffuse and infiltrative growth combined with florid microvascular proliferation and pseudopalisading necrosis (Tolnay, 2002). These are the histopathological characteristics that are unique to highly malignant tumors. GBM may have more than one focus, due to spreading of tumor cells through the cerebrospinal fluid, white matter tracts or meninges. Due to its high grade of malignancy GBM is considered a Grade 4 tumor by the WHO (Louis et al., 2007).

Different cell types that may predominate in GBM include fibrillary cells, spindle cells, gemistocytes, small cells or giant cells (Ohgaki & Kleihues, 2005).

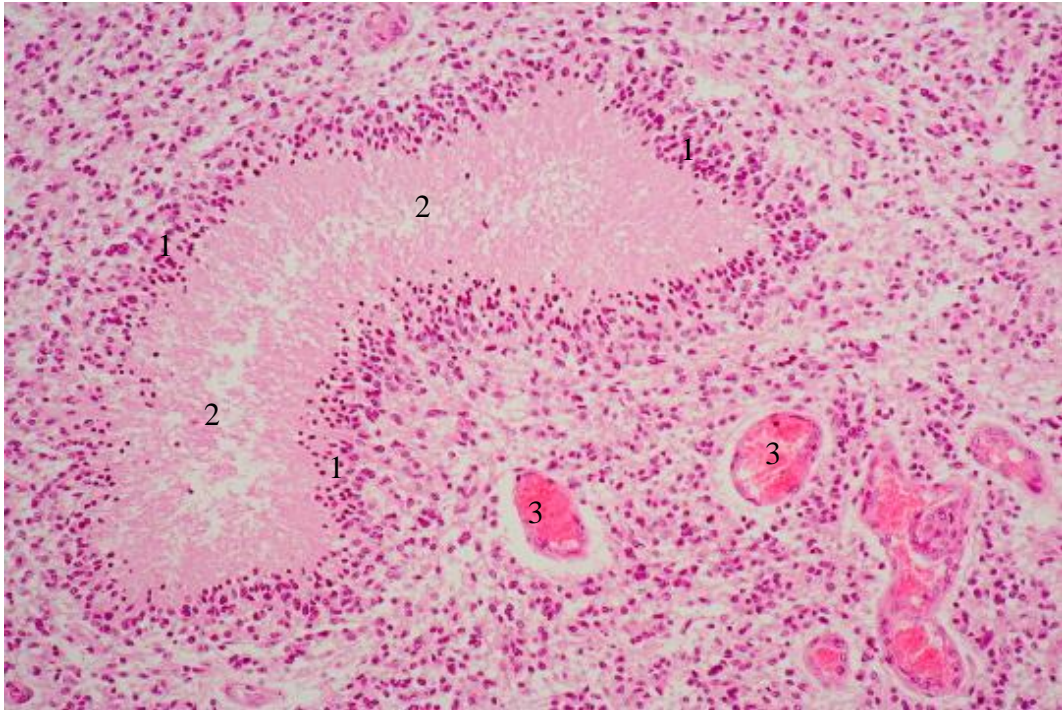


Figure 1: Histopathology of Glioblastoma showing pseudopalisading(1) with necrosis(2) of neoplastic cells along with microvascular proliferation(3) (source: [webpath.med.utah.edu](http://webpath.med.utah.edu), accessed on 01.06.2022)

### 3.1.3 Localization and clinical presentation

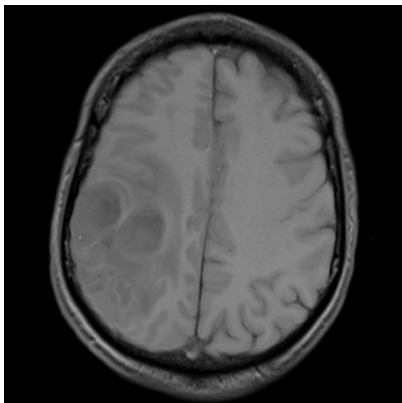
GBM is located usually in the frontal or temporal lobes of cerebral hemispheres (Roux et al., 2019), a combined frontotemporal Location is also typical. Gliomas are more often unifocal than multifocal (Omuro, 2013). This neoplasm can also arise very rarely in the brain stem and cerebellum (Stark, Maslehaty, Hugo, Mahvash, & Mehdorn, 2010).

The clinical presentation differs according to tumor localization. A focal neurologic deficit suggests the localization in or around the corresponding eloquent region, when GBM is diagnosed in a patient due to epileptic seizures, the localization is mostly the temporal lobes (Roux et al., 2019). The mean duration of preceding clinical symptoms in patients with primary GBM was 6.3 months and thus significantly shorter compared to 16.8 months in secondary GBM (Ohgaki & Kleihues, 2007). Occasionally the symptoms may develop rapidly,

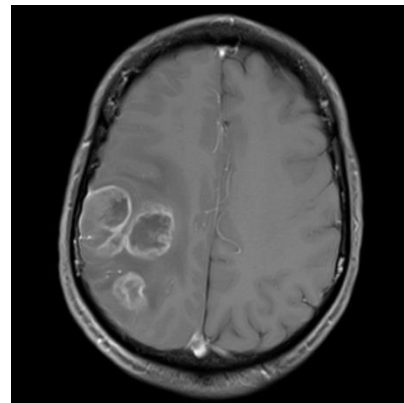
which might be mistaken for a stroke. Other symptoms include headache, visual disturbances, incontinence or ataxia (Omuro, 2013).

### 3.1.4 Imaging and Diagnosis

The routinely used non-invasive imaging techniques for visualizing brain tumors are computed tomography (CT) and magnetic resonance imaging (MRI) (Nelson, 2003). In clinical setting T1 weighted, T2 weighted and gadolinium-enhanced sequences of MRI play a pivotal role in the diagnosis and treatment follow up of gliomas (Upadhyay et. al, 2011). In an MR scan enhanced with Gadolinium GBMs show irregular enhancement, central area of necrosis, and surrounding white matter oedema (Nelson, 2003). An MRI enhanced with Gadolinium is also routinely performed within 72 hours of surgery to assess the extent of tumor resection more accurately (Albert, Forsting, Sartor, Adams, & Kunze, 1994; Forsting et al., 1993). Surgically induced contrast enhancements make this Assessment difficult as time progresses after surgery (Bette et al., 2016; Lescher, Schniewindt, Jurcoane, Senft, & Hattingen, 2014). A postoperative MRI also helps exclude complications such as bleeding or stroke.



A



B

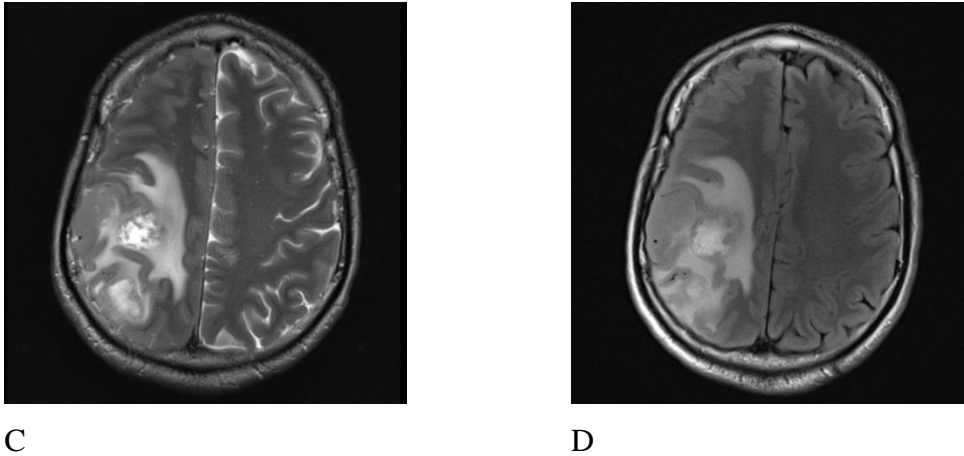


Figure 2: Different MRI modalities of a female patient aged 55 with multifocal GBM - T1 weighted (A), T1-weighted enhanced with Gadolinium (B), T2 weighted (C), FLAIR (D). (Department of Neurosurgery, Klinikum Deggendorf)

This 58 year old female patient had been suffering from significant problems with fine motor skills of her left hand and from increasing numbness of the distal left arm for about 3 weeks when she sought medical help. In addition, she also had right sided headaches. The MRI of the head (Figure 2) revealed multiple cystic lesions in the right parietal lobe (A) with marginal Gadolinium enhancement (B). T2 weighted imaging (C) and FLAIR or Fluid-attenuated inversion recovery sequence (D) showed considerable vasogenic edema around the lesions. Biopsy of the microsurgically removed tumor confirmed Glioblastoma.

Advanced nuclear medicine imaging techniques such as single photon emission computed tomography (SPECT) and positron emission tomography (PET) can tell apart active tumor from therapy-related changes (Nelson, 2003). Diffusion Tensor Imaging (DTI) is a technique that helps map white matter tracts in the brain that are clinically relevant. This information can be of immense help in planning safer surgical approaches for removal of tumors that have proximity to eloquent regions of the brain (González-Darder et al., 2010). In cases where neurosurgical resection is not possible, a biopsy is performed. Definitive diagnosis is based on histopathological examination of the surgically removed tumor tissue.

### **3.1.5 Molecular markers**

The most important molecular markers routinely determined for GBM are isocitrate dehydrogenase gene (IDH) and methyl-guanine methyl transferase gene (MGMT).

Mutations in the IDH gene 1 or 2 in GBM suggests that it is secondary in origin or developed from a lower grade Glioma (Hartmann et al., 2013). Around 5% of GBM patients carry IDH mutation and are thus secondary. The patients diagnosed with secondary GBM are usually much younger with a median age of 32 years compared to those with primary GBM with a median age of 59 years. Patients with secondary GBM also have a significantly better prognosis with a median overall survival of 31 months, in comparison to around 15 months in primary GBM with wild-type IDH1 (Yan et al., 2009).

O6-methylguanine methyltransferase (MGMT) is a protein that repairs DNA. Its causes fast reverse alkylation at the O6 position of guanine, this neutralizes the cytotoxic effects of alkylating agents such as temozolomide (TMZ) (Pegg, Dolan, & Moschel, 1995). MGMT methylation reduces the capability of the tumor cells to fix the damage caused to the DNA from chemotherapy, thus leading to a better response when treated with TMZ (Hegi et al., 2008). MGMT Promotor methylation is associated with improved overall survival in general and significantly longer progression free survival (Wang, Song, Zha, & Li, 2016)

### **3.1.6 Therapy**

Usually the aim of surgery is the complete resection of tumors, but the diffuse growth of gliomas in the brain parenchyma makes a complete removal impossible. As early as 1928, neurosurgeons noticed that even after performing a hemispherectomy, patients with diffuse glioma were not cured (Dandy, 1928). Modern neurosurgical procedures, in particular fluorescence-assisted resection



with the aid of 5-aminolevulinic acid (ALA), enable complete resection of the tumor on a macroscopic level in many cases (Stummer et al., 2008).

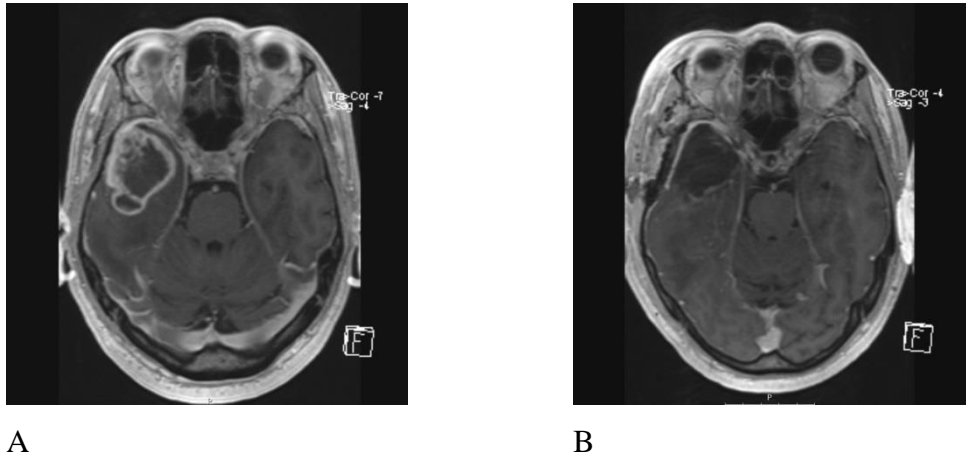


Figure 3: preoperative (A) and postoperative (B) axial Gadolinium-enhanced T1-weighted MR images of a 60 year old male (Department of Neurosurgery, Klinikum Deggendorf)

An MRI was performed in the above patient when he presented after a seizure, he had also been suffering from psychological changes with depressive episodes and restlessness for the last 2 months. The scan showed an inhomogeneous lesion in the right temporal lobe measuring approximately 3cm x 4cm with marginal contrast enhancement typical for high grade Gliomas (Figure 3 A). The tumor could be surgically removed completely as shown in B. Biopsy of the removed tumor revealed Giant-cell Glioblastoma.

In 2005 Stupp and his colleagues made the break through discovery that the addition of TMZ to radiotherapy increased the two-year survival rate of GBM patients from 10.4 % to 26.5 % as compared to radiotherapy alone. The additional toxicity from this treatment was minimal. Since then tumor resection to a maximum extent possible without worsening neurological impairment followed by radiotherapy with concomitant and maintenance TMZ has been adopted worldwide as standard for GBM treatment (Stupp et. al., 2014).

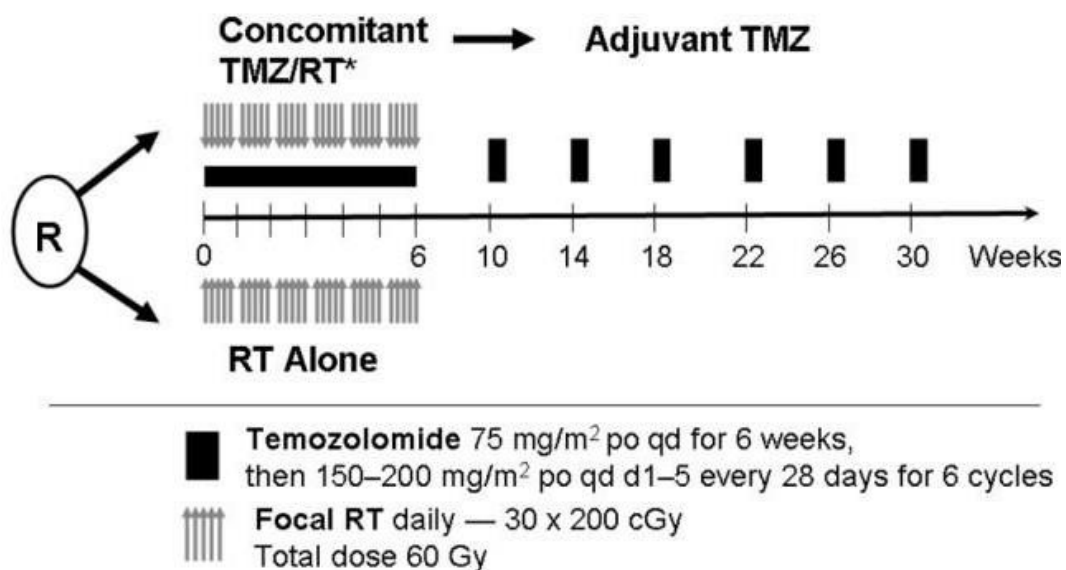


Figure 4: Stupp Regimen (Gilbert and Armstrong 2007)

Stupp regimen: As illustrated in Figure 4, after surgical resection once the wound is healed, fractionated focal irradiation is commenced at 2 Gray (Gy) daily for 5 days per week for 6 weeks, for a total of 60 Gy. In addition, the patient receives 75 mg/m<sup>2</sup> (mg per square meter body surface area) temozolomide daily for this duration. After this concomitant phase a 4 week break follows. Then the patients are administered six cycles of adjuvant temozolomide at 150 to 200 mg/m<sup>2</sup> for 5 days during each 28-day cycle.

### 3.1.7 Other therapeutic Approaches

#### 3.1.7.1 Bevacizumab

GBM has extensive abnormal vasculature. Vascular endothelial growth factor (VEGF) is the prominent protein responsible for angiogenesis in these tumors (Schmidt et al., 1999). Bevacizumab is a humanized monoclonal antibody that inhibits VEGF-A protein thus curbing angiogenesis. Treatment of recurrent GBM with this drug improves the PFS significantly, moreover it has an anti-edematic effect and thus may have quality of life benefits (Kreisl et al., 2009; Vredenburgh et al., 2010)

### 3.1.7.2 Tumor treating field therapy

Tumor treating fields (TTFields) are a non-invasive mode of therapy aimed at augmenting the already existing treatment for glioblastoma and other cancers. It involves the administration of low-intensity alternating electric fields at a frequency of 100-500 kilohertz (kHz) via transducer arrays placed on the scalp or skin close to the tumor. These fields exert biophysical force on active tumor cells disrupting mitosis (Kirson et al., 2004). A randomized clinical trial showed that the use of TTFields in combination with maintenance TMZ chemotherapy improves the progression-free survival and overall survival significantly in comparison to maintenance TMZ alone (Roger Stupp et al., 2017). But the TTFields has to be administered continuously, for at least 18 hours per day for significantly longer median overall survival (Toms, Kim, Nicholas, & Ram, 2019).

### 3.1.7.3 Immunotherapeutic concepts

Immunotherapy has revolutionized the treatment of numerous cancer types such as melanoma (Waldman, Fritz, & Lenardo, 2020), metastatic renal cell cancer (Rini et al., 2019) etc. There are several ongoing trials and researches exploring innovative immune-targeting strategies in GBM.

Rindopepimut is a peptide cancer vaccine administered through injection. It brings forth a strong immune response against GBM cells that express epidermal growth factor receptor variant III (EGFRvIII). EGFRvIII is a mutated protein present in about 25% of GBM patients. Although the results seemed promising in Phase 2 trial, the Phase 3 trial was stopped after it proved futile in an interim analysis. No significant overall survival advantage was found compared to the control group (Weller et al., 2017).

Another area of research is the development of oncolytic viruses engineered to selectively infect GBM cells. Some of these viral vectors such as vocimagene

amiretrorepvec (Toca 511) and flucytosine (Toca FC) have also been in randomized clinical trials but did not improve survival of GBM patients (Cloughesy et al., 2020).

Checkpoint blockade inhibitors which in essence limit the inhibition of T lymphocytes by cancer cells have shown good survival benefits in tumors such as melanoma (Mahoney, Freeman, & McDermott, 2015). A such drug Nivolumab has been tested in Phase 3 trials in GBM patients but no survival benefits could be seen (Reardon et al., 2020).

Adoptive cell transfer with chimeric antigen receptor T cells (CAR-T cells) which are genetically engineered T cells capable of recognizing tumor cells without the help of MHC have shown promising results in first 2 phases of clinical trials. Phase 3 trial results are yet to be published (Li et al., 2020).

As discussed above, immunotherapy in GBM is yet to make a clinical breakthrough.

### **3.1.8 Prognosis and factors affecting prognosis**

The median overall survival of 14.6 months, 2 year survival of 26.5% and 5 year survival of 9.7% is a dismal outcome in GBM patients, despite being subjected to the maximum therapy of surgery followed by concomitant radiochemotherapy and maintenance chemotherapy (Roger Stupp et al., 2005). Age, Karnofsky performance status score, extent of resection, and the degree of necrosis and enhancement on preoperative MRI studies are 5 independent predictive factors which influence prognosis of GBM patients (Lacroix et al., 2001).

## **3.2 Immune system**

The human immune system has 3 levels of defence mechanisms of increasing specificity. The first lines of defence are the physical and chemical barriers such

as skin and hair or mucous membrane and body fluids with its enzymes. Microbes that successfully evade these barriers then face the next line of defence which is called the innate immune system. This is a non-specific response which is triggered when certain receptors detect molecules specific to microbes. These 'pattern recognition receptors' are found in dendritic cells, macrophages, monocytes, neutrophils and epithelial cells. The detected pathogens are then eliminated by phagocytosis. Another form of innate immune response is inflammation caused by the release of certain chemicals from the infected cells which attract more immune cells to the site of infection.

Next is the specific or acquired immune response, which is built based on memory of earlier infections or immunological memory. It is constituted by the B lymphocytes and T lymphocytes which are readily activated when a known antigen causes an infection again. This mechanism thus helps the immune system adapt during the course of an individual's life.

### **3.2.1 Immune system vs cancer**

Since long ago scientists have known that certain bacterial infections can trigger an immune response causing a cancer-suppressive effect. William Coley was among the first in modern times to observe and document this phenomenon. He observed long-term regression in patients with inoperable sarcoma after injecting them with heat-inactivated bacteria (Coley WB, 1893). In 1976 a bacterium *Bacillus Calmette-Guérin* (BCG) was found to be effective in treating superficial bladder cancer (Morales, Eidinger, & Bruce, 1976). Furthermore spontaneous regression of malignant tumors has been well documented although this happens rarely at around 1 in every 60,000 to 100,000 cancer cases (Kucerova & Cervinkova, 2016).

The transformation of a normal cell into a malignant phenotype due to mutation triggers intrinsic cell death pathways. One of the 6 hallmarks of cancer (Figure 5) is its ability to evade this programmed immune destruction.

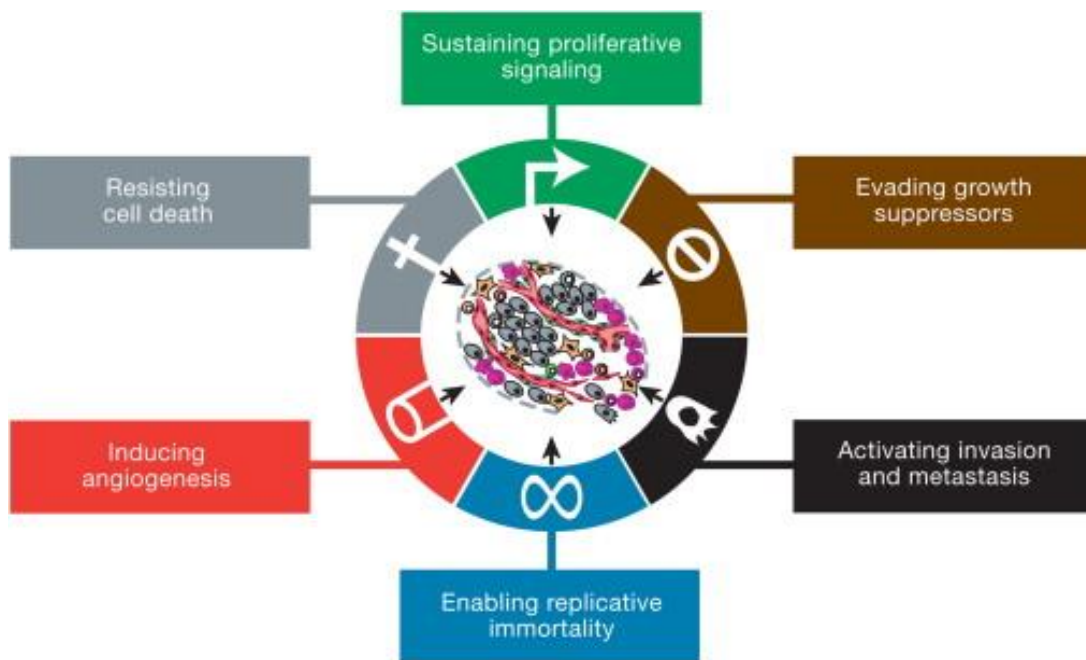


Figure 5: Hallmarks of cancer (Hanahan and Weinberg 2011)

Cancers have a heterogeneous environment made of tumor cells, immune cells, fibroblasts, and pericytes. This niche constitutes the tumor microenvironment (TME). Our immune system is capable of detecting and destroying cancerous cells by different means, this is referred to as immune surveillance. Many of the immune cells that are part of immune surveillance polarise into pro-tumorigenic cells, depending on signals derived from cancer cells and their microenvironment leading to its progress (Wellenstein & de Visser, 2018). A better understanding of how immune system reacts to cancers and how cancers overcome the defensive mechanisms are crucial in optimizing the existing therapy.

Immunotherapy focused on TILs in the TME has gained a lot of importance in the last decade. TILs are the second most common of the immune cells found in the TME in humans after tumor associated macrophages. They can trigger inflammatory or anti-inflammatory processes in the TME (Speiser, Ho, & Verdeil, 2016). One common type of TIL found in the TME is cytotoxic CD8<sup>+</sup> T cells. Their function is to kill cells that are infected, dysfunctional or malignant. Antigen

presenting cells (APCs) display tumor antigens on their surface bound by major histocompatibility complex I (MHC 1) protein. They are equipped with T cell receptors that recognize these complexes and thus get activated. When activated they release a set of cytotoxins inducing apoptosis (Barnes & Amir, 2017). Higher density of CD8+ T lymphocytes in the TME is known to be a positive prognostic factor in many malignancies such as ovarian cancer (Hwang, Adams, Tahirovic, Hagemann, & Coukos, 2012), HER-2 positive breast cancer (Salgado et al., 2015), metastatic melanoma (Erdag et al., 2012), head and neck squamous cell carcinoma (Balermipas et al., 2016) etc..

FoxP3+ Tregs are another specialised group of T lymphocytes that play an inevitable role in immunological self-tolerance preventing autoimmune diseases. A number of tumors have a high number of Tregs in their TME. Higher concentration of Tregs has shown to negatively influence the prognosis in melanoma and in cancers of breast, kidney and cervix (Shang, Liu, Jiang, & Liu, 2015). On the contrary some studies have shown that higher density of Tregs relate to better prognosis in patients with Hodgkin lymphoma and colorectal cancer (Álvaro et al., 2005; Salama et al., 2009).

Cancer evades the immune system either by avoiding the immune recognition or by creating an immunosuppressive TME. For example, avoidance of immune recognition by CD8+ cytotoxic T cells may be achieved through mutations or deletions that partially inhibit the antigen presentation mechanisms (Patel et al., 2017). Similarly immunosuppressive TME may also be created by inducing the recruitment of Tregs by tumor-derived chemokines (Tanaka & Sakaguchi, 2017) or by secretion of suppressive molecules such as IL-10, TGF- $\beta$  etc. (Domínguez-Soto et al., 2011; Massagué, 2008).

The disruption in the integrity of the blood-brain barrier and the blood-cerebrospinal fluid barrier under pathological circumstances as in a brain tumor helps the inflammatory cells to enter the brain. This explains the TIL activity seen

in brain tumors despite the immune privilege it is known to possess (Sevenich, 2019)

#### **4 Abstract**

Since the introduction of Stupp protocol about 17 years ago that significantly raised the two-year survival rate of GBM patients to 26.5 percent as compared to 10.4 percent with radiotherapy alone there has not been any further development that turned out advantageous to the patients apart from the vascular endothelial growth factor antibody, bevacizumab, that could prolong progression-free, but not overall survival. Over the last few decades the interaction between cancers and immune system has been a subject of intense research. With regard to GBM, the most notorious of the central nervous system tumors, this opens up new doors, which could lead to the development of an effective immunotherapy that improves survival and quality of life of patients.

In our study we analyzed the impact of two subgroups of TILs, namely the CD8+ cytotoxic T cells and the FoxP3+ regulatory T cells on the prognosis in GBM. Tumor specimens from 104 GBM patients treated in Klinikum Lichtenfels and Klinikum Bayreuth between 2002 and 2014 were studied. The tumor microenvironment was divided into 5 different ROI based on microscopic characteristics. The CD8+ and FoxP3+ TILs were stained using a double staining method and then counted semi automatically supported by the software “Biomass-Count”. Thus a topographical understanding of the immunological structure in tumor microenvironment in each ROI was obtained. Then Kaplan-Meier plots were constructed correlating TIL density and survival.

We found out that the CD8+ cells are present in a much larger number as compared to FoxP3+ cells in each ROI. The density of each cell type didn't vary much between the 4 ROI containing tumor (tumor core, necrosis, infiltration zone and peripheral zone). The normal brain tissue adjacent to tumor showed significantly lesser number of both these subgroup of TILs. Only the density of



CD8+ TIL in the tumor core was found to be of prognostic significance in our study. The patients with a lower CD8+ cell density than the median seemed to have a better overall survival ( $p=0.028$ ).

## **5 Method**

### **5.1 Studied glioblastoma cohort**

We collected tumor samples from 104 GBM patients who were treated in Klinikum Lichtenfels and Klinikum Bayreuth between 2002 and 2014. 43% of the patient population was females and the rest males. The median age at diagnosis was 66.8 years, average age at diagnosis was 65 years, the youngest patient was 36 years old and the oldest 85.4 years. The KPS score of these patients at diagnosis ranged from 30% to 100% with the mean and median at 70%. All the patients underwent surgery. A total resection of tumor was achieved in 25% of the patients. Most tumors were localized in the temporal (36%), frontal (26%) and parietal lobes (13%). Other localizations were occipital lobe (9%), brain stem (4%) and multifocal (2%). The distribution between the two hemispheres was approximately equal. 82 patients received adjuvant RCT, 9 received radiotherapy, the rest did not receive further treatment after surgery.

The data was provided by Tumorzentrum Oberfranken and the remaining study relevant patient information was retrieved to the maximum extend possible from the archives of Klinikum Lichtenfels and Klinikum Bayreuth.

### **5.2 Production of the tissue microarrays (TMA)**

Tissue microarray is a technique in which tiny tissue cores are removed from biopsy samples with a hollow needle and then assembled on a single receiver block, the microarray, at precise array coordinates. A schematic presentation of this process is depicted in Figure 6.

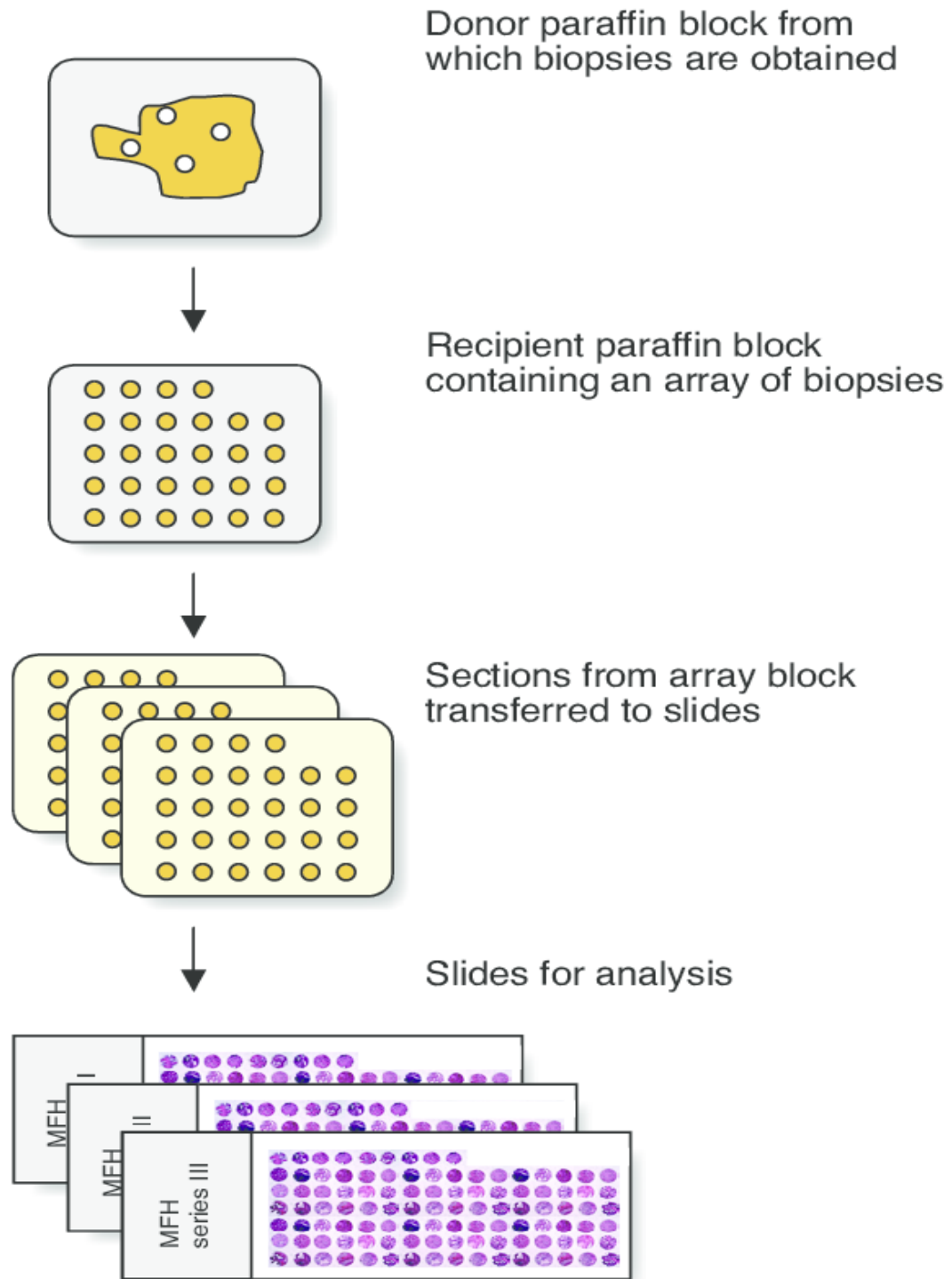


Figure 6: Schematic presentation of the tissue microarray method. (Nilbert and Engellau, 2004)

The tissue samples embedded in paraffin (donor blocks) and the corresponding haematoxylin and eosine-stained (HE) sections were provided by the two

previously mentioned treatment centres. The HE sections were evaluated under a light microscope and 5 regions of interest (ROI): central tumor, necrosis zone, infiltration zone, peripheral zone and normal brain tissue around tumor were marked. These served as a template and helped identify the respective areas on the donor blocks, which were removed from the donor block using a hollow needle and reassembled in TMA blocks. In total 104 cores could be taken from tumor cores, 69 from the necrotic zone, 64 from the infiltration zone, 86 from the peripheral zone and 34 tissue cores from adjacent normal tissue. TMAs were made from a total of 352 tissue punches

### **5.3 Immunohistochemical staining**

A double immunostaining method was employed to identify and differentiate the FoxP3+ Tregs and CD8+ cytotoxic T cells. The biotin-streptavidin complex method was used for CD8 staining. For FoxP3 staining the same method had to be reinforced with tyramine.

First, a thin tissue section (3 $\mu$ m) was cut from the TMA paraffin block. This TMA tissue section was mounted on a slide and was repeatedly rinsed with xylene and ethanol solutions in different concentrations to remove the paraffin. First three xylene solutions were allowed to act on the TMA sections for ten minutes each. They were then placed twice in 100% ethanol solution for two minutes each, twice in 96% ethanol solution for two minutes each and finally in 70% ethanol solution for two minutes. Then the TMA sections were put in a cuvette with citric acid buffer that consisted of 2.1g citric acid in 1000ml double distilled water at a pH of 6.0. The next step was antigen unmasking. For this the cuvette containing the sections were heated in distilled water in a pressure cooker at 120°C for five minutes. After this one litre of TRIS buffer solution containing one millilitre of TWEEN was sprinkled onto a Cuver plate. The slides are then placed on the cover plate with the sections facing down, making sure no air bubbles formed and transferred to a rack box and filled with TRIS / TWEEN buffer. After the buffer

solution had drained, 5 drops of blocking solution 1 was added. This was allowed to act for 5 minutes and then rinsed with TRIS / TWEEN buffer solution. Then a solution of FoxP3 protein antibody and albumin in a ratio of 1:200 was added and stored overnight. Next day the chambers were rinsed again with TRIS / TWEEN solution, 5 drops of Post Block Reagent 2 were then applied. This was allowed to act for 20 minutes after which the slides were rinsed again with TRIS / TWEEN solution. 5 drops of AP polymer 3 (Zytomed, Berlin, Germany) was then applied. After half an hour, it was rinsed one more time with TRIS / TWEEN solution and then 3 drops of Fast Red were applied to each slide and covered for 20 minutes. Rinsing the slides under running water and transferring them to a cuvette filled with distilled water completed the initial process of staining. The first step in the latter part of the double staining was to boil the slides in a citrate buffer with a pH of 6.0. This was done using a microwave. The next step was placing them in a solution of the containing CD8 antibody and albumin in a ratio of 1:50 and then rinsing with the TRIS / TWEEN solution. A drop of Brij (polyalkylene glycol ether), was then added and incubated for half an hour in a solution containing the antibody against CD8. This followed the rinsing of the slides again with TRIS / TWEEN solution, after which they were kept in a strept-AB complex. After a rinse with TRIS / TWEEN solution, the slides were then stained with Fast Blue. This followed a last rinsing in running water. They were then kept in distilled water. Then they were counterstained with hematoxylin and finally covered in an aqueous medium.

## **5.4 Analysis**

The TMAs were digitized using the MIRAX scanner manufactured by Zeiss. A program called 3Dhistech used for panoramic viewing was then used to crop the TMAs into smaller subunits. These cropped images were compressed and saved. The further optimization of these compressed graphic formats and the counting of the cells were carried out using the semiautomatic program called Biomas Count (Prof. Dr. Luitpold Distel, Erlangen, Germany). The program could automatically identify and count the cells based on inputs regarding size, shape and color. A

manual correction at the end of this work step was possible which further increased the accuracy. The program then created an Excel table containing all the data.

#### **5.4.1 Cell counts and cell density**

In order to obtain the cell density, the absolute number of cells was first counted and set in relation to the area under consideration. Biomax calculated the relative cell density per mm<sup>2</sup> from the absolute number of cells counted in each case, taking into account the previously defined "region of interest" (ROI) i.e. the central tumor tissue, the necrosis zone, the infiltration zone of the tumor, the tumor periphery and parts of the adjacent normal tissue in glioblastomas were examined.

#### **5.4.2 Statistics**

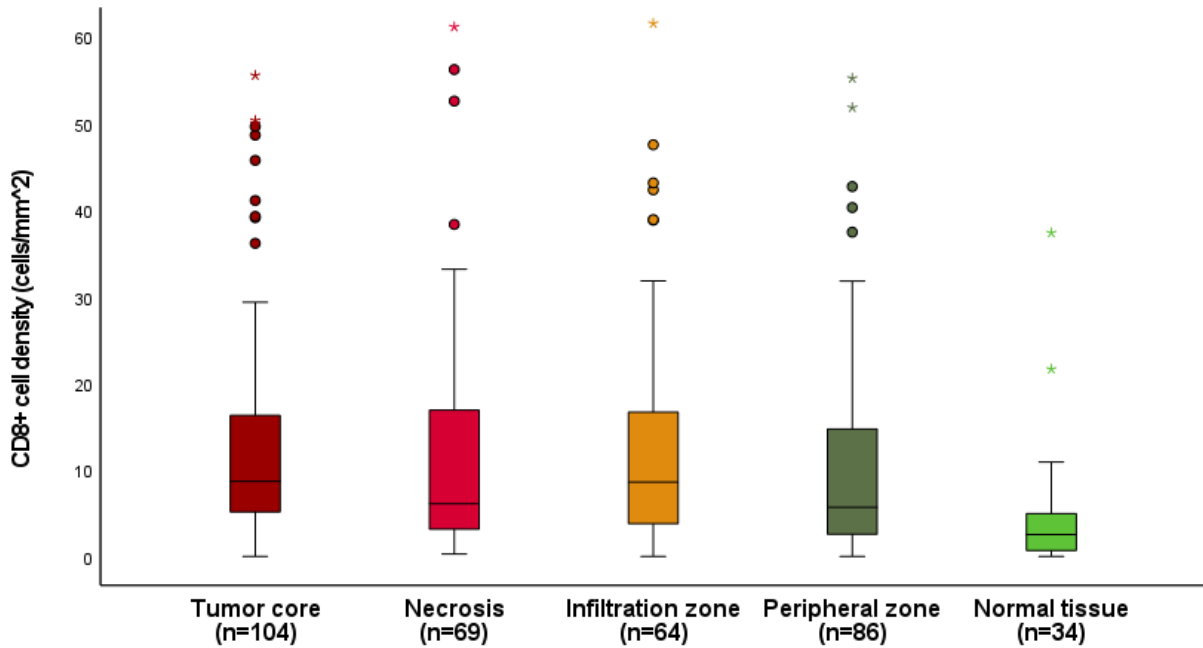
SPSS Statistics Version 22 (IBM, Armonk - New York, USA) was used to carry out statistical analysis of the data. The variation in the distribution of Tregs and CD8+ cells between the ROI were analyzed by comparing the median cell density using T test for independent variables, for which a significance level of  $p < 0.05$  was given. Box plots were constructed using the data obtained. The median cell densities of CD8+ cells and Tregs were also compared in each ROI.

In order to find the correlation between the survival rates and the cell density, the patient population was split into two groups based on the median of cell density that was calculated for each ROI for both cell types. While group "0" showed a cell density below the median, group "1" contained the rest with density equal to or higher than the median. The log-rank test was then performed to compare the two survival curves. Thus correlation diagrams for each ROI comparing the – Kaplan-Meier plots for both overall and progression free survival were constructed.

## 6 Results

### 6.1 Immune cell density

#### 6.1.1 Density of CD8+ Lymphocytes in the 5 ROI

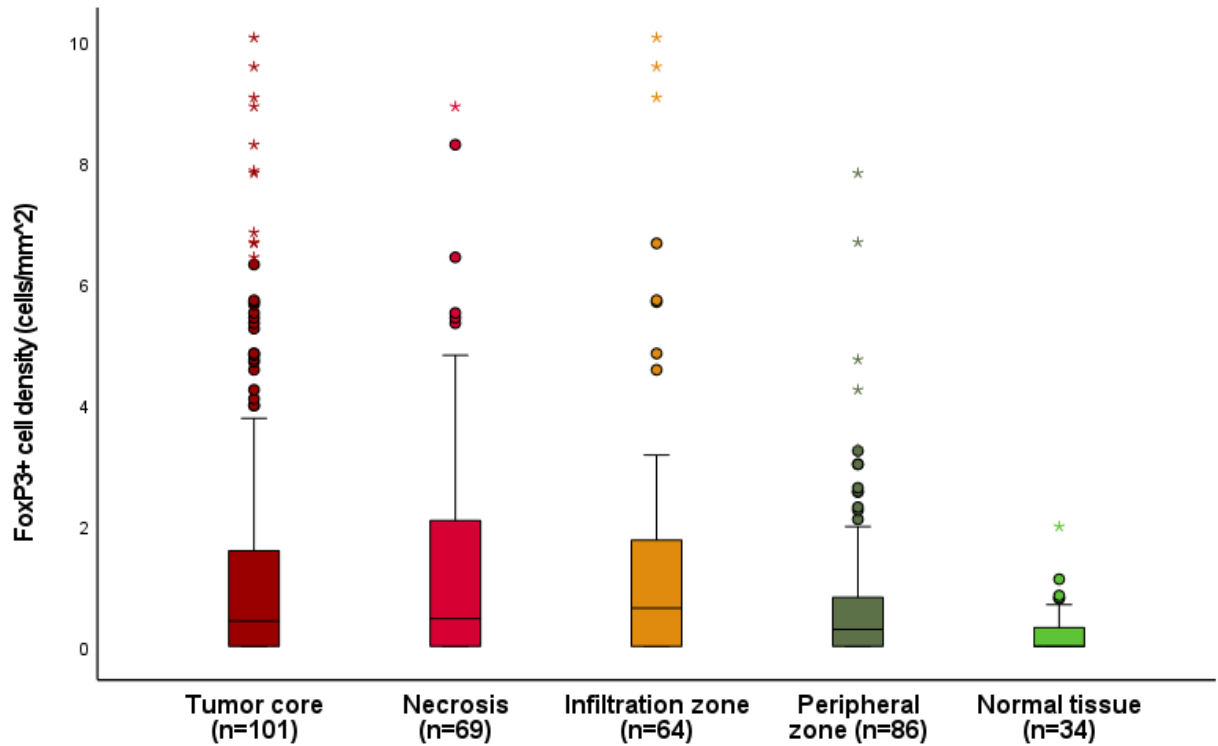


Circles: Outliers between 1.5x and 3x IQR; Stars: Outliers > 3x IQR; 13 Outliers are not shown

Figure 7: Box plot depicting the cell density in cells/mm<sup>2</sup> of CD8+ TILs. The median cell density seems to drop from the tumor core towards the normal tissue except for an increase in the infiltration zone.

As shown in Figure 7, the median density of CD8+ cells was the highest at the tumor core (6.3 cells/mm<sup>2</sup>) followed by necrotic zone (6.1 cells/mm<sup>2</sup>), peripheral zone (5.7 cells/mm<sup>2</sup>) and normal tissue adjacent to tumor (2.5 cells/mm<sup>2</sup>) respectively. The infiltration zone showed the highest median cell density of CD8+ TILs at 8.6 cells/mm<sup>2</sup>. However cell density was shown not to vary significantly between 4 different regions containing tumor in t-tests. But the normal tissue surrounding the tumor seems to have significantly fewer cells per mm<sup>2</sup> compared to the other 4 ROI ( $p < 0.005$ ).

### 6.1.2 Density of FoxP3+ Lymphocytes in the 5 ROI



Circles: Outliers between 1.5x and 3x interquartile range(IQR); Stars: Outliers > 3x IQR; 12 Outliers are not shown

Figure 8: Box plot depicting the cell density in cells/mm<sup>2</sup> of FoxP3+ TILs. The median cell density seems to drop from the tumor core towards the normal tissue except for a slight increase in the infiltration zone.

Figure 8 compares the median densities of Tregs in the different ROI. The median density of Tregs was also the highest at the tumor core (0.8 cells/mm<sup>2</sup>) followed by necrosis (0.5 cells/mm<sup>2</sup>), peripheral zone (0.3 cells/mm<sup>2</sup>) and normal tissue (0 cells/mm<sup>2</sup>) respectively. The infiltration zone showed slightly higher median cell density than necrotic zone at 0.6 cells/mm<sup>2</sup>.

Similar to CD8+ cells, the cell density was again shown not to vary significantly between 4 different regions containing tumor. The normal tissue surrounding the tumor obviously had a significant difference compared to the other 4 ROI in t-tests ( $p \leq 0.005$ )

### 6.1.3 Comparison of mean cell density-es of CD8+ and FoxP3+ Lymphocytes

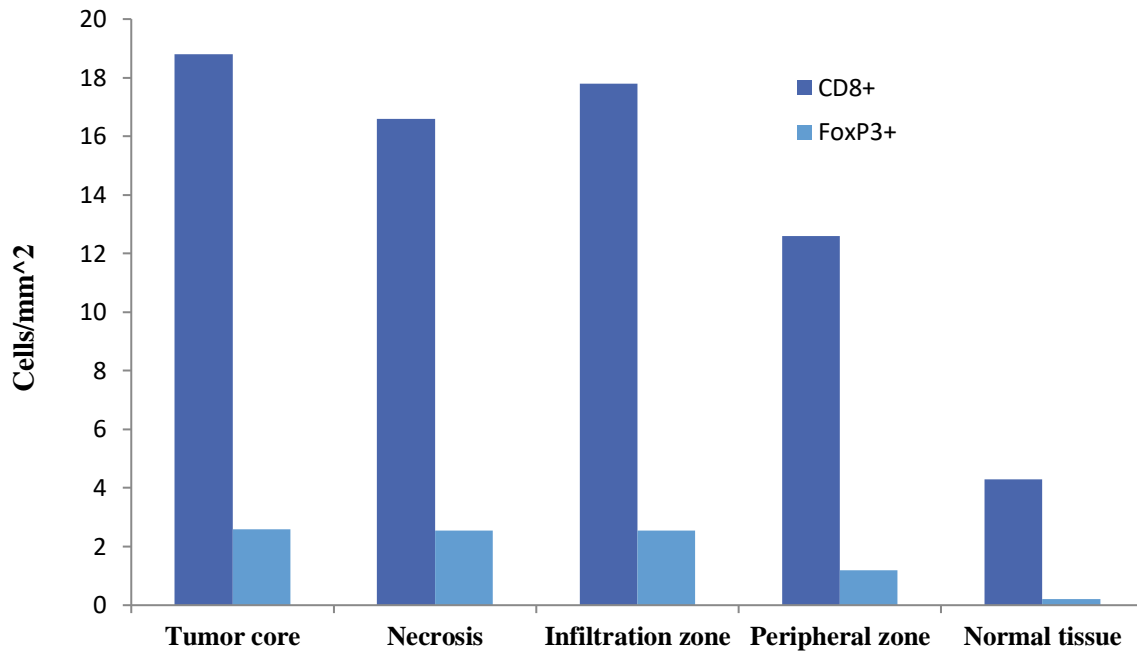


Figure 9: Here the mean cell densities of the CD8+ TILs are compared with FoxP3+ TILs in the different ROI.

It is evident from the above graph (Figure 9) that the mean cell density of CD8+ cells is much higher in each ROI as compared to that of Tregs. The mean cell density seems to decrease with increasing distance from the tumor core except in the infiltration zone which seems to have a slightly higher mean cell density than necrotic zone for both subtypes of TILs.



### 6.1.4 Correlation between cell density and survival

The possible association between the density of CD8+ and FoxP3+ TILs with overall survival and progression free survival was analysed with the help of Kaplan-Meier plots and log rank tests. Following observations were made for CD8+ Cells:

#### 1. CD8+ cell density at tumor core and overall survival

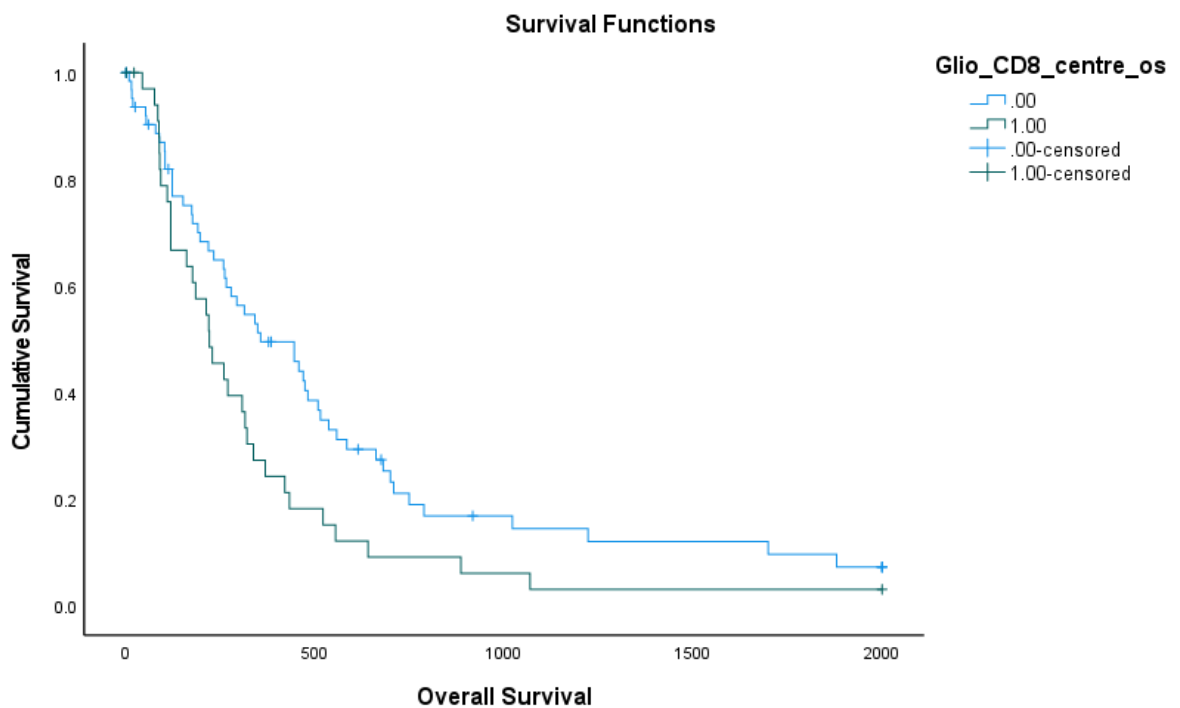


Figure 10: Density of CD8+ cells per mm<sup>2</sup> at tumor core in relation to overall survival in days after surgery (p=.028). Green line: group with higher cell density than median, blue line: group with lower cell density than median.

The above Kaplan-Meier plot (Figure 10) compares the overall survival of patients having a high density of CD8+ T cells at the tumor core with that of the patients with a low density CD8+ T cells at the tumor core observed over a period of 2000 days (~5.5 years). The patients with a lower cell density seem to have a better overall survival (p=0.028).

2. CD8+ cell density at tumor core and progression free survival

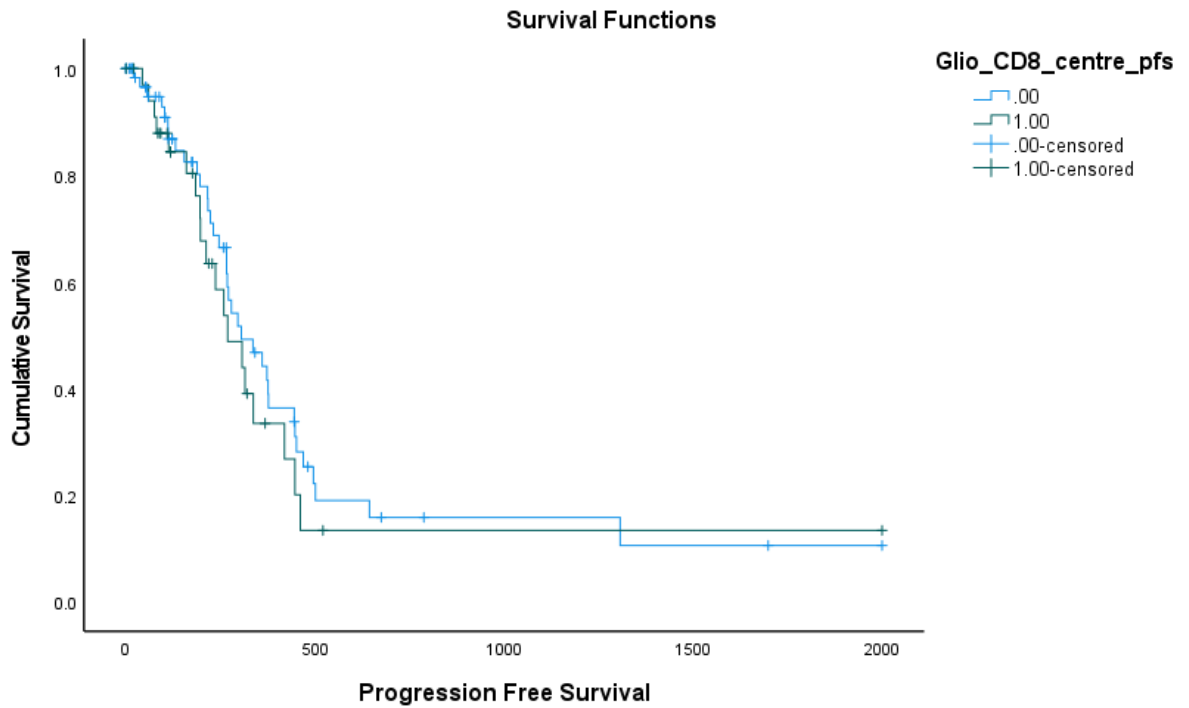


Figure 11: Density of CD8+ cells (per mm<sup>2</sup>) at tumor core in relation to progression free survival in days from surgery (p= .471). Green line: group with higher cell density, blue line: group with lower cell density

Figure 11 compares the progression free survival of patients having a high density of CD8+ cytotoxic T cells at the tumor core with that of the patients with a low density CD8+ cytotoxic T cells at the tumor core observed over a period 5.5 years. No significant differences were observed (p=0.471).

### 3. CD8+ cell density in tumor necrosis and overall survival

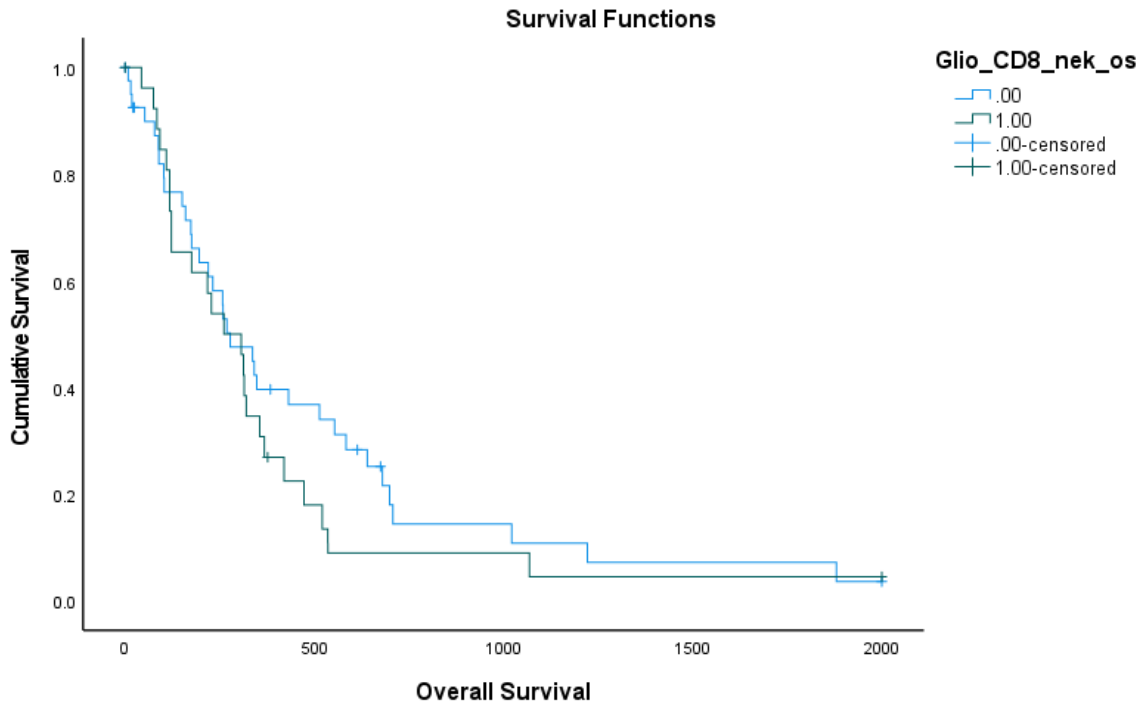


Figure 12: Density of CD8+ cells (per mm<sup>2</sup>) in tumor necrosis in relation to overall survival in days (p= .364). Green line: group with higher cell density, blue line: group with lower cell density.

Figure 12 compares the overall survival of GBM patients having a high density of CD8+ cytotoxic T cells at the tumor necrosis with that of the patients with a low density CD8+ cytotoxic T cells at the tumor necrosis observed over a period of 5.5 years. No significant differences were observed (p=0.364).

4. CD8+ cell density in tumor necrosis and progression free survival

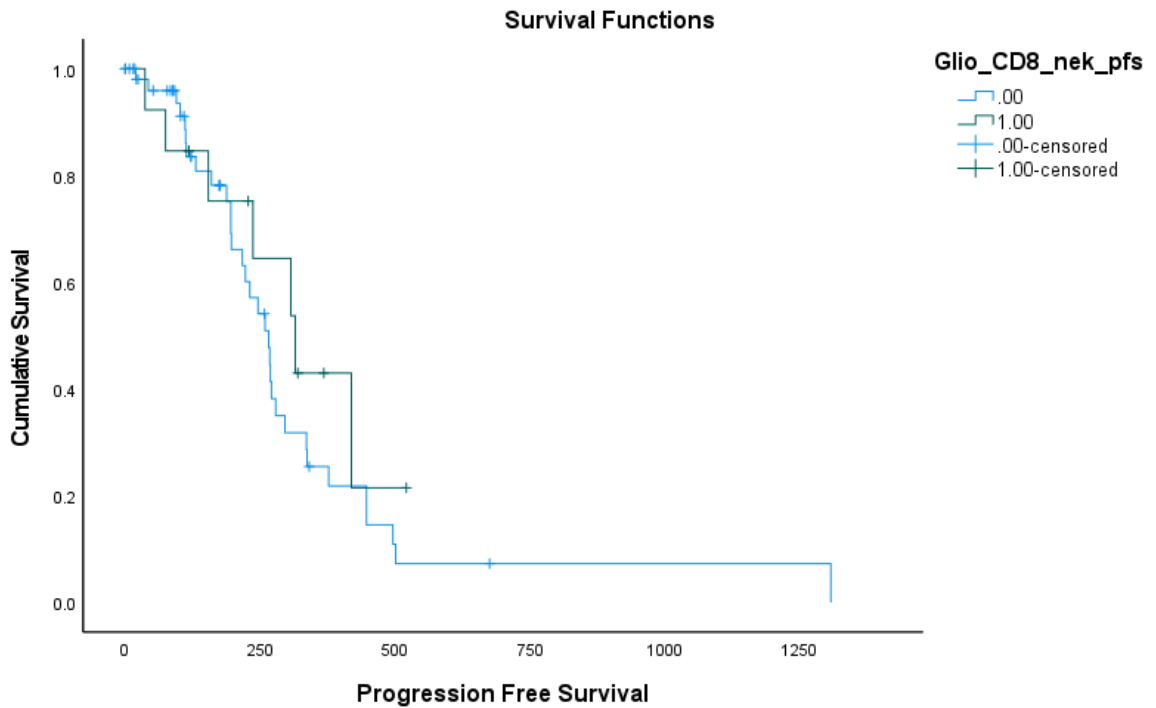


Figure 13: Density of CD8+ cells (per mm<sup>2</sup>) in tumor necrosis in relation to progression free survival in days (p= .350). Green line: group with higher cell density, blue line: group with lower cell density

Figure 13 compares the progression free survival of the two groups of GBM patients divided on the basis CD8+ cytotoxic T cell density in tumor necrosis at median. No significant differences were observed (p=0.350).

5. CD8+ cell density in infiltration zone and overall survival

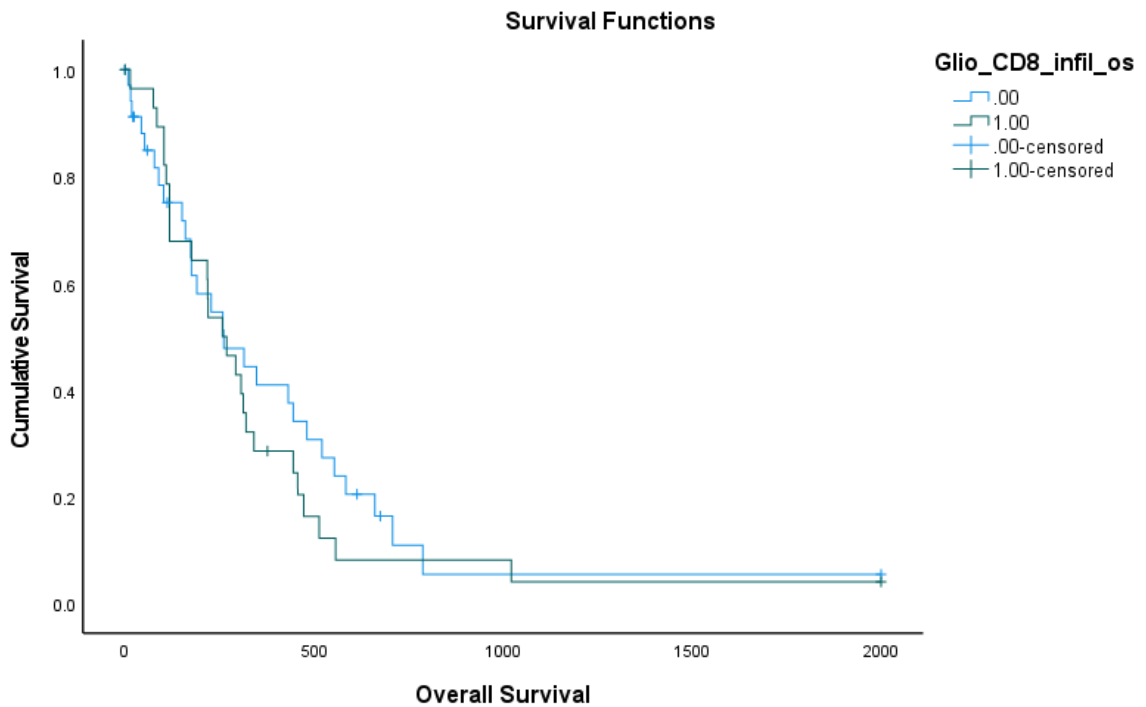


Figure 14: Density of CD8+ cells (per mm<sup>2</sup>) in infiltration zone in relation to overall survival in days (p= .492). Green line: group with higher cell density, blue line: group with lower cell density

The above Kaplan-Meier plot (Figure 14) compares the overall survival of patients having a higher density of CD8+ cytotoxic T cells in the infiltration zone with that of the those with a low density CD8+ cytotoxic T cells at the infiltration zone observed over a period of 2000 days (~5.5 years). No significant differences can be noted (p=0.492), although at two years the patients with a lower cell density seem to have a survival advantage.

6. CD8+ cell density in infiltration zone and progression free survival

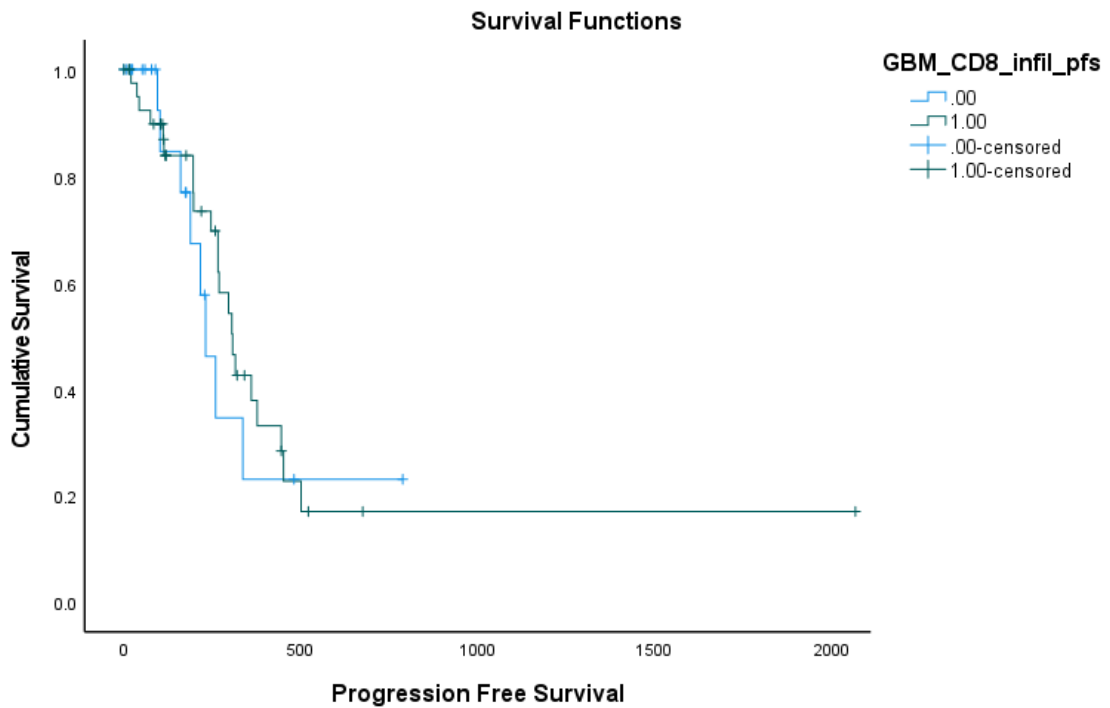


Figure 15: Density of CD8+ cells (per mm<sup>2</sup>) in infiltration zone in relation to progression free survival in days (p=.617). Green line: group with higher cell density, blue line: group with lower cell density

The comparison of the progression free survival of GBM patient groups divided on the basis of CD8+ cell density at median (Figure 15) didn't show any significant differences (p=.617).

7. CD8+ cell density in peripheral zone and overall survival

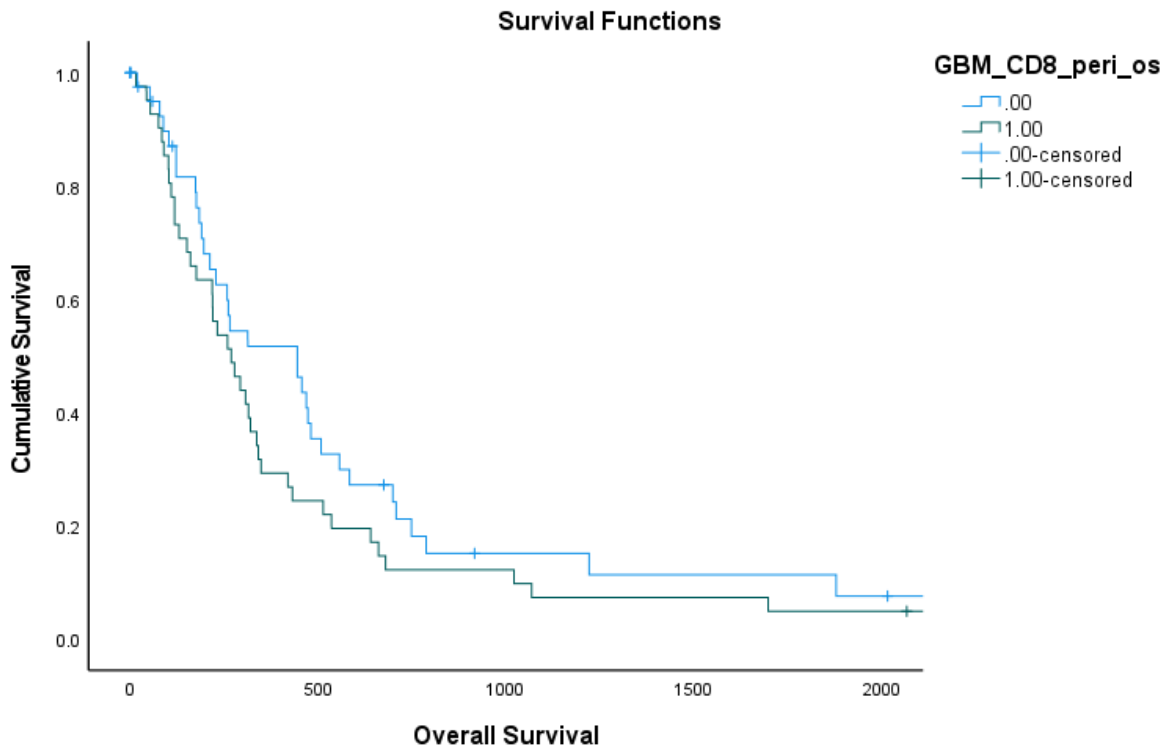


Figure 16: Density of CD8+ cells (per mm<sup>2</sup>) in peripheral zone in relation to overall survival in days (p=.191). Green line: group with higher cell density, blue line: group with lower cell density

Figure 16 shows the overall survival of GBM patients having a high density of CD8+ cytotoxic T cells compared to that of the patients with a low density of CD8+ cytotoxic T cells in the peripheral zone of the tumor observed over a period of 2000 days (~5.5 years). No significant differences were observed (p=0.191).

8. CD8+ cell density in peripheral zone and progression free survival

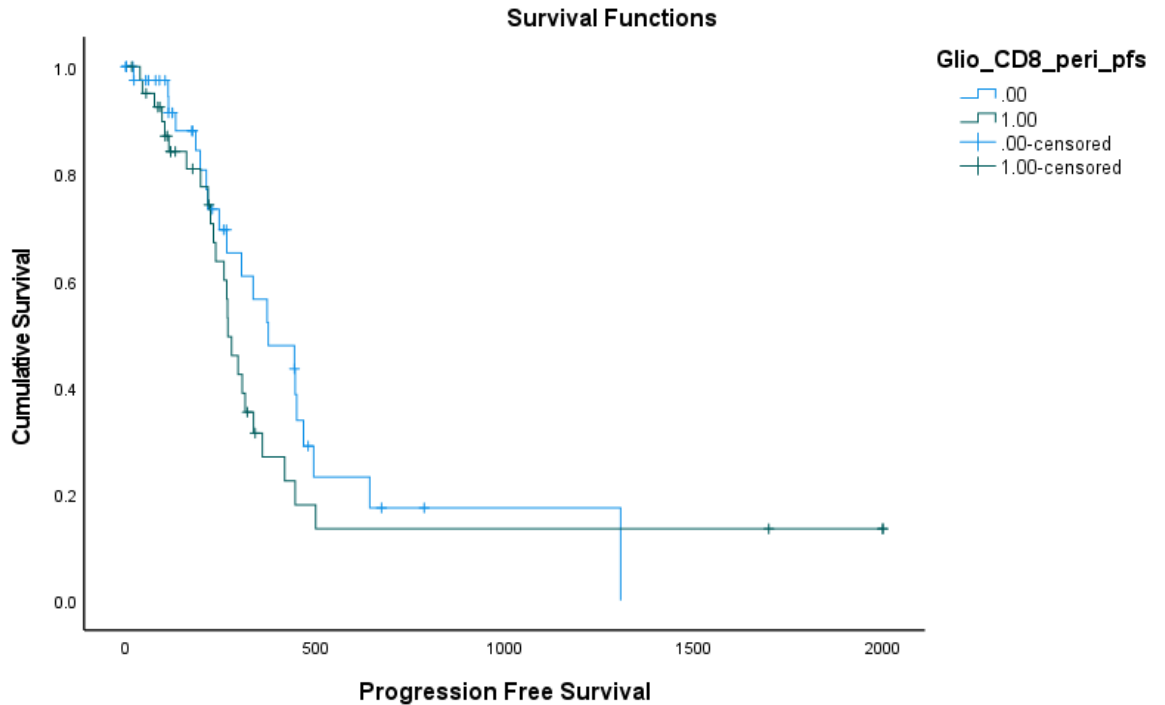


Figure 17: Density of CD8+ cells (per mm<sup>2</sup>) in peripheral zone in relation to progression free survival in days (p= .294). Green line: group with higher cell density, blue line: group with lower cell density

Figure 17 shows the progression free survival of GBM patients having a high density of CD8+ cytotoxic T cells compared to that of the patients with a low density of CD8+ cytotoxic T cells in the peripheral zone of the tumor observed over a period of 2000 days. No significant differences were observed (p=0.294).



9. CD8+ cell density in normal tissue and overall survival

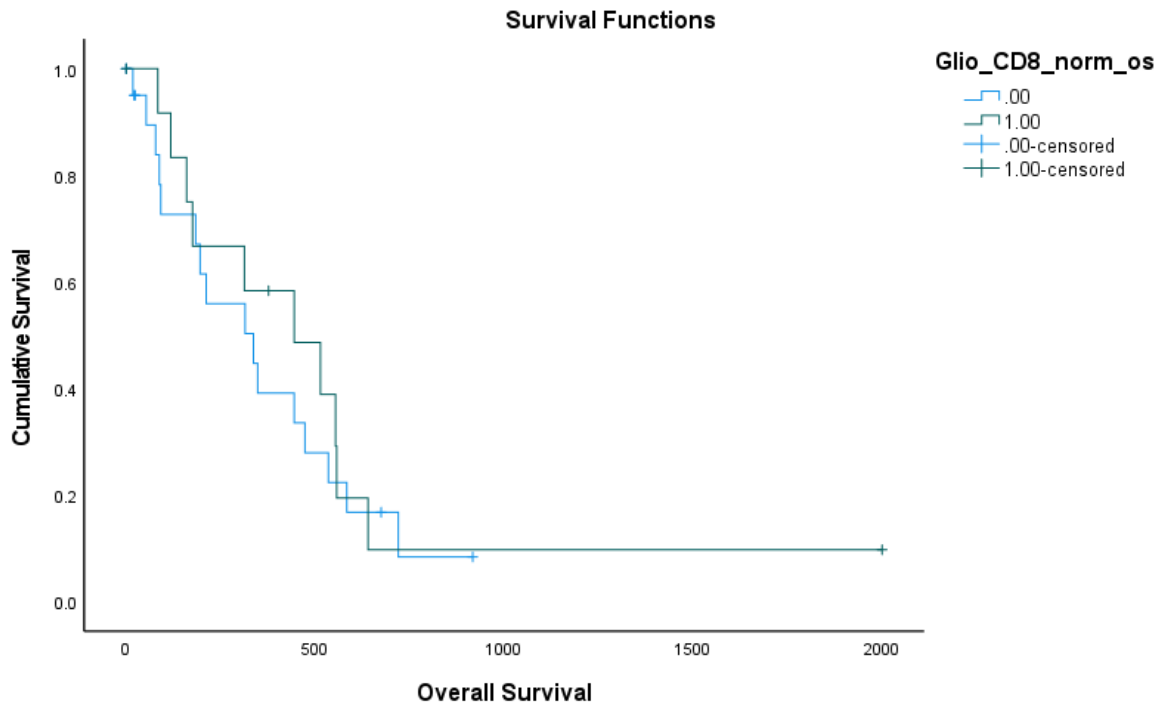


Figure 18: Density of CD8+ cells (per mm<sup>2</sup>) in normal tissue in relation to overall survival in days (p= .659). Green line: group with higher cell density, blue line: group with lower cell density

In this Kaplan-Meier plot (Figure 18) the overall survival of GBM patients having a high density of CD8+ cytotoxic T cells in the normal tissue adjacent to tumor is compared to that of the patients with a low density of these cells in the same region. No significant differences were noted (p=.659).

## 10. CD8+ cell density in normal tissue and progression free survival

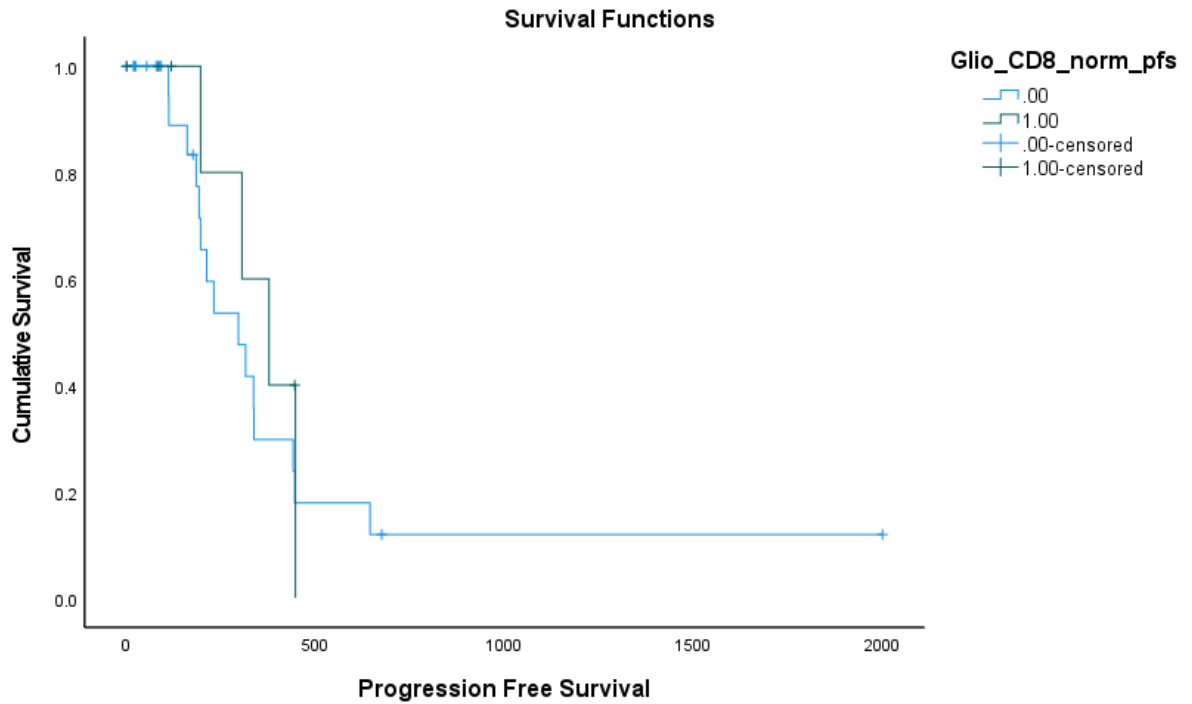


Figure 19: Density of CD8+ cells (per mm<sup>2</sup>) in normal tissue in relation to progression free survival after surgery in days (p= .523). Green line: group with higher cell density, blue line: group with lower cell density

Figure 19 depicts the variation in the progression free survival of patients having a high density of CD8+ cytotoxic T cells in the normal tissue adjacent to tumor compared to that of the patients with a low density of these cells in the same region. No significant differences were noted (p=.523).

Following observations were made for FoxP3+ Cells:

1. FoxP3+ cell density in tumor core and overall survival

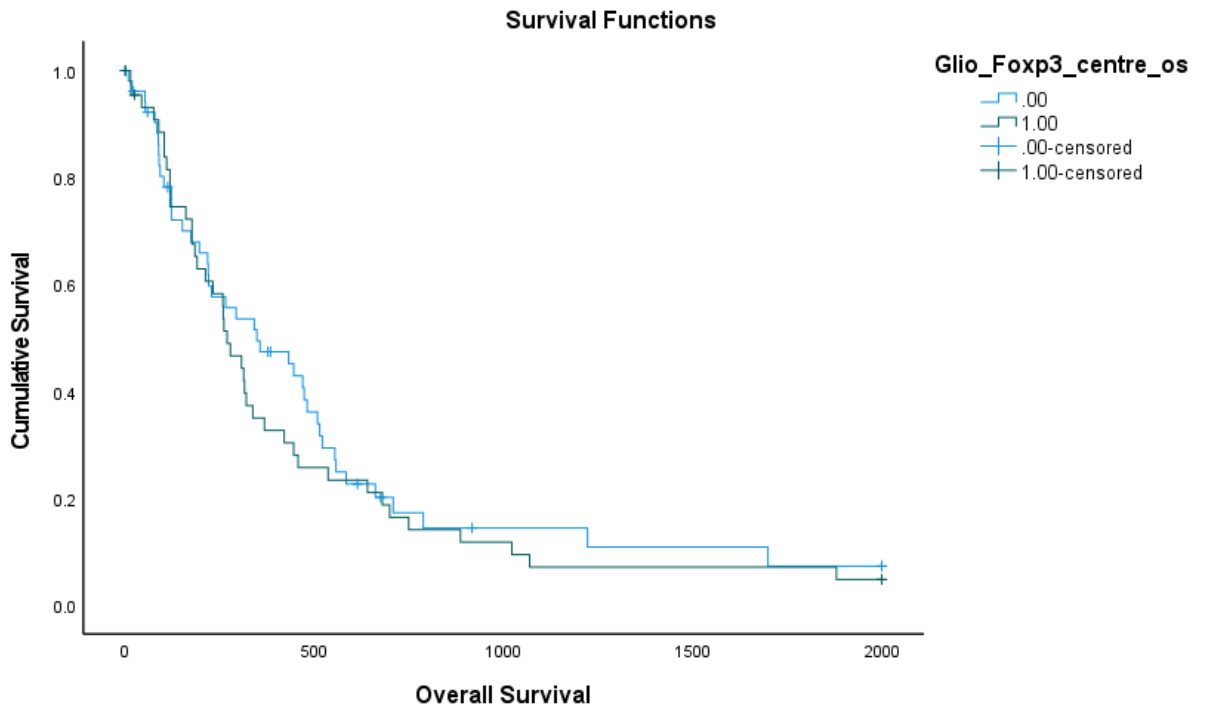


Figure 20: Density of FoxP3+ cells (per mm<sup>2</sup>) in tumor core in relation to overall survival in days from surgery (p= .501). Green line: group with higher cell density, blue line: group with lower cell density

Figure 20 compares the overall survival of GBM patients having a high density of FoxP3+ regulatory T lymphocytes to that of the patients with a low density of FoxP3+ regulatory T lymphocytes at the tumor core observed over a period of 2000 days (~5.5 years). No significant differences were noted (p=0.501).

2. FoxP3+ cell density in tumor core and progression free survival

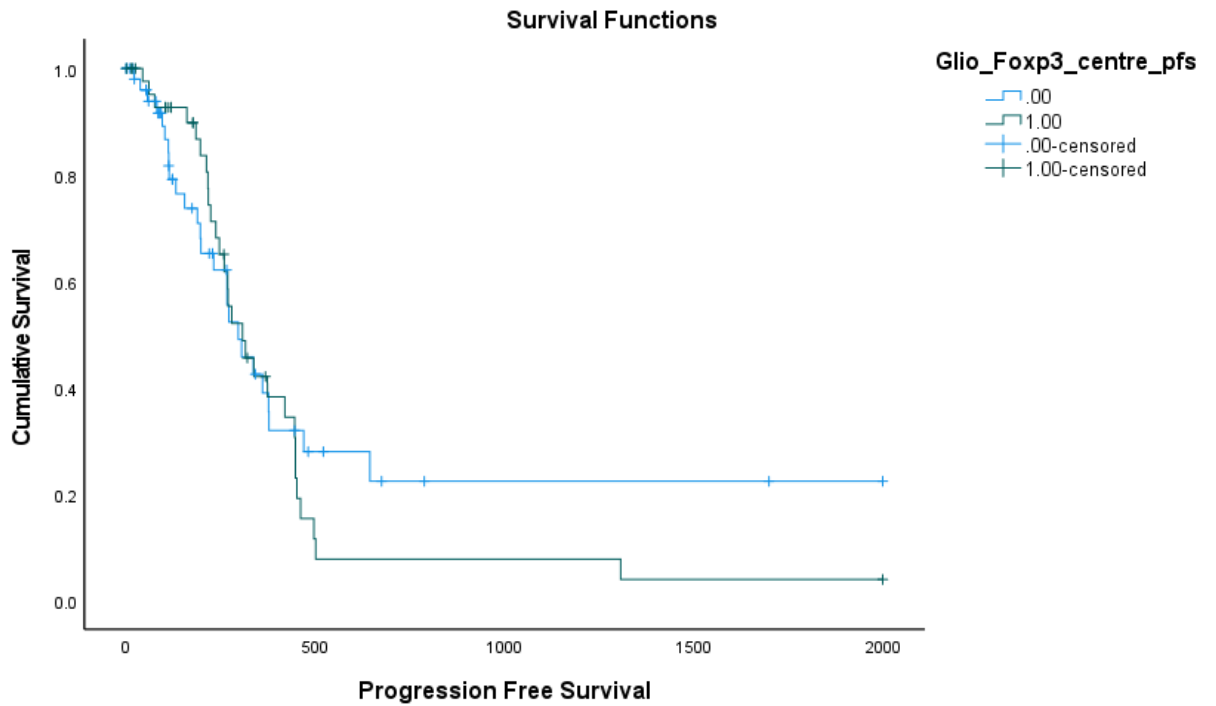


Figure 21: Density of FoxP3+ cells (per mm<sup>2</sup>) in tumor core in relation to progression free survival in days from surgery (p= .594). Green line: group with higher cell density, blue line: group with lower cell density

Figure 21 compares the progression free survival of GBM patients having a high density of FoxP3+ regulatory T lymphocytes to that of the patients with a low density of FoxP3+ regulatory T lymphocytes at the tumor core. The tendency is that the patients with a lower cell density have a progression free survival at 2 years from surgery, but this variation was not shown to be significant (p=0.594).

### 3. FoxP3+ cell density in tumor necrosis and overall survival

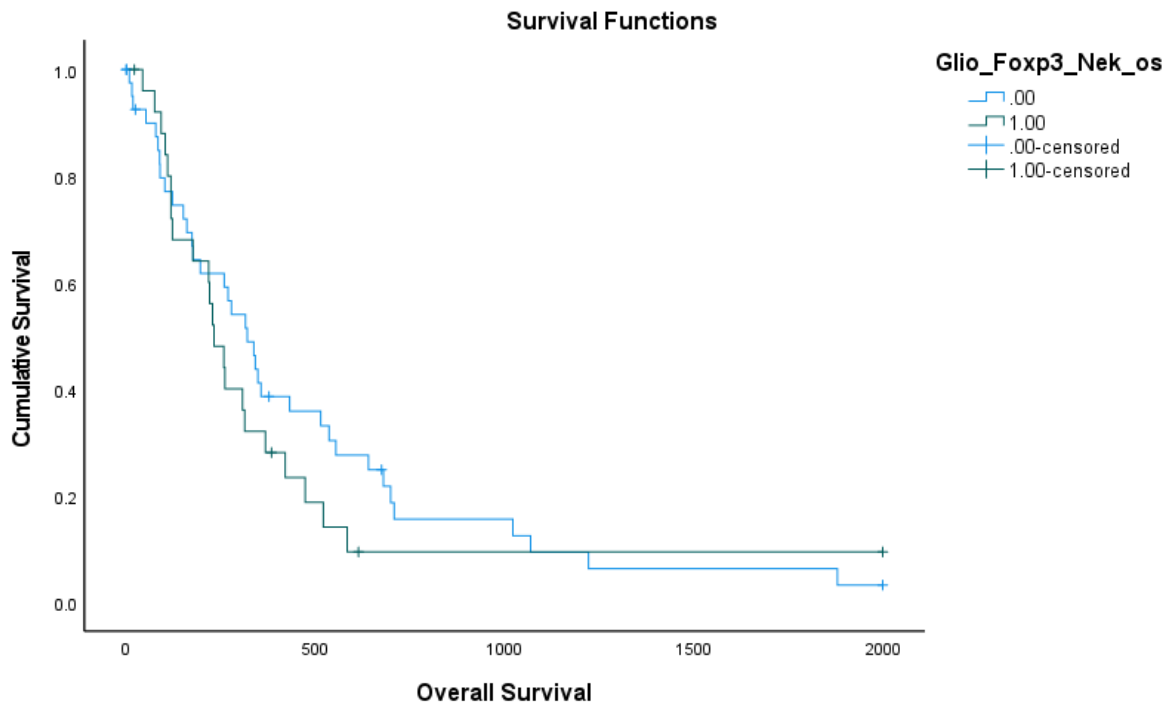


Figure 22: Density of FoxP3+ cells (per mm<sup>2</sup>) in tumor necrosis in relation to overall survival in days from surgery (p= .370). Green line: group with higher cell density, blue line: group with lower cell density

The above Kaplan-Meier (Figure 22) plot compares the overall survival of patients having a higher density of Tregs in tumor necrosis with that of the those with a low density of Tregs in the necrosis observed over a period of 2000 days (~5.5 years). No significant differences were noted (p=0.370), although at 500 days from surgery the patients with a lower cell density seem to have a survival advantage.

#### 4. FoxP3+ cell density in tumor necrosis and progression free survival

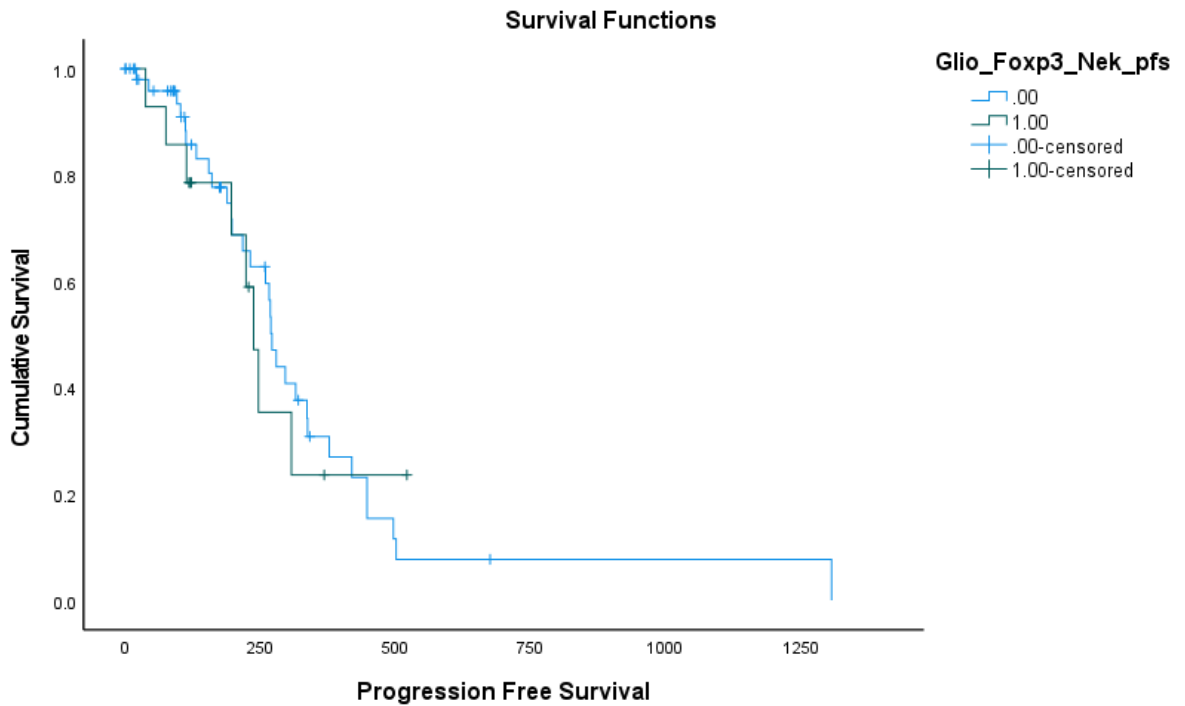


Figure 23: Density of FoxP3+ cells (per mm<sup>2</sup>) in tumor necrosis in relation to progression free survival in days from surgery (p= .807). Green line: group with higher cell density, blue line: group with lower cell density

This curve (Figure 23) depicts the differences in the progression free survival of GBM patients having a high density Tregs in the necrosis compared to that of the patients with a low density of these cells in the same region. No significant differences were noted (p=0.807).

5. FoxP3+ cell density in infiltration zone and overall survival

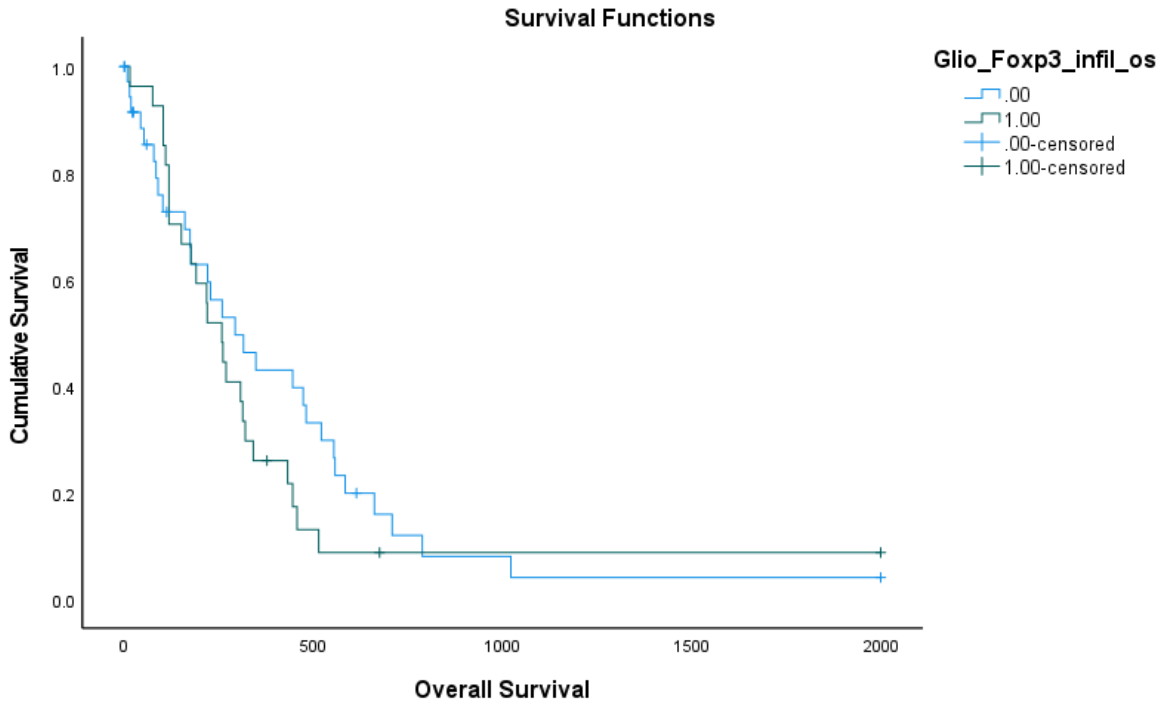


Figure 24: Density of FoxP3+ cells (per mm<sup>2</sup>) in the infiltration zone relation to overall survival in days from surgery (p= .360). Green line: group with higher cell density, blue line: group with lower cell density

Figure 24 is a Kaplan-Meier plot that compares the overall survival of patients having a higher density Tregs in the infiltration zone with that of the those with a low Tregs in the infiltration zone observed over a period of 2000 days (~5.5 years). No significant variation was seen (p=0.360).

6. FoxP3+ cell density in infiltration zone and progression free survival

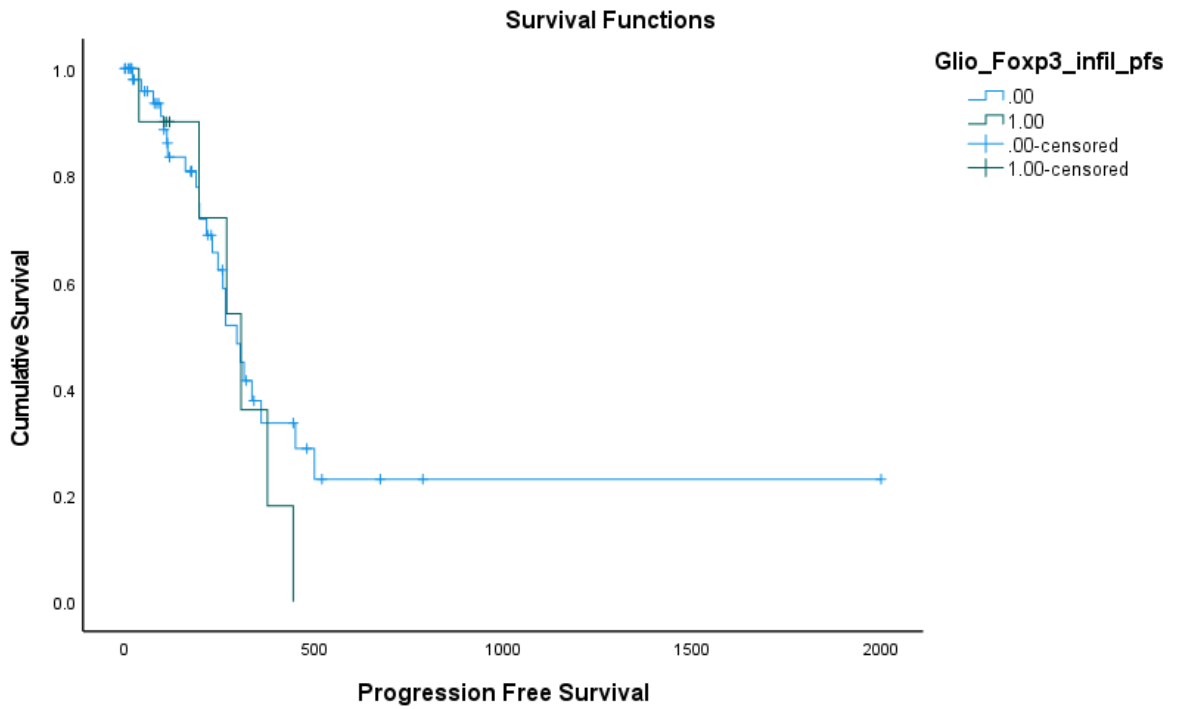


Figure 25: Density of FoxP3+ cells (per mm<sup>2</sup>) in the infiltration zone relation to progression free survival in days from surgery (p= .522). Green line: group with higher cell density, blue line: group with lower cell density

The comparison of the progression free survival of GBM patient groups divided on the basis of Treg cell density at median (Figure 25) didn't show any significant differences either (p=.522).



7. FoxP3+ cell density in peripheral zone and overall survival

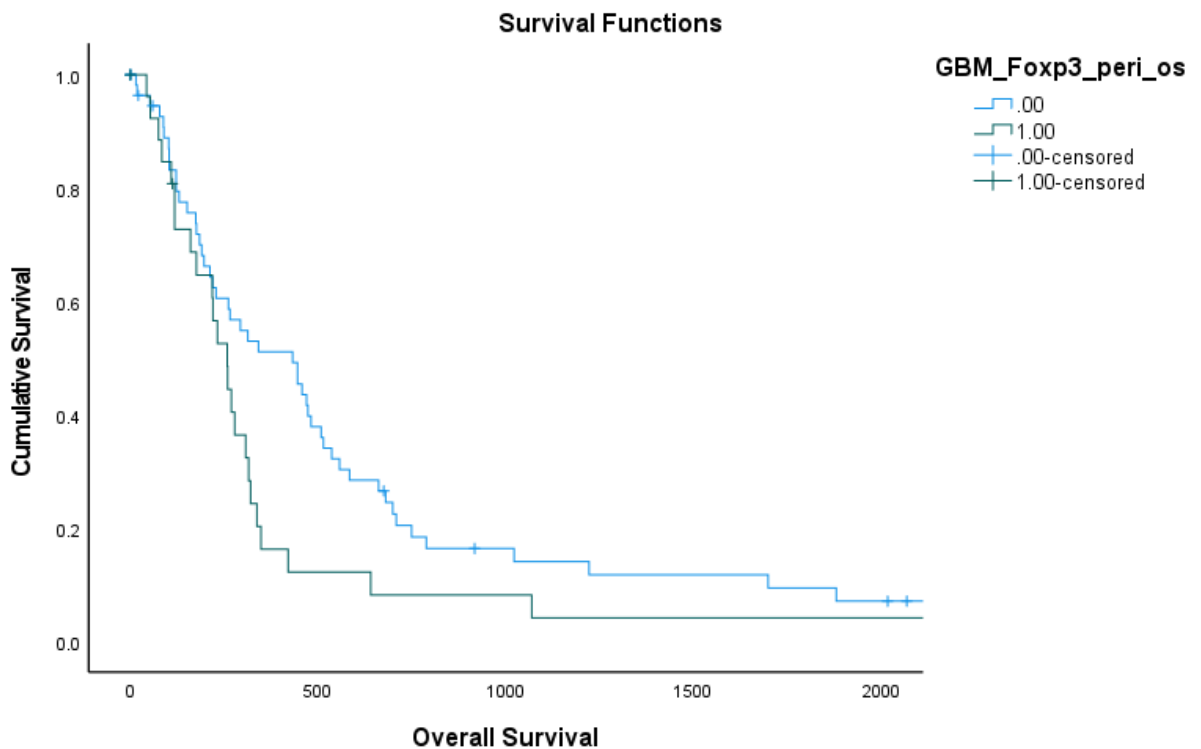


Figure 26: Density of FoxP3+ cells (per mm<sup>2</sup>) in the periphery in relation to overall survival in days from surgery (p= .054). Green line: group with higher cell density, blue line: group with lower cell density

Figure 26 compares the overall survival of GBM patients having a high density of Tregs to that of the patients with a low density of Tregs in the peripheral zone of the tumor observed over a period of 2000 days (~5.5 years). The differences were not significant (p=0.054). But at around 2 years from surgery, the GBM Patients with a lower density of Tregs in the infiltration zone seem to have a survival advantage.

8. FoxP3+ cell density in peripheral zone and progression free survival

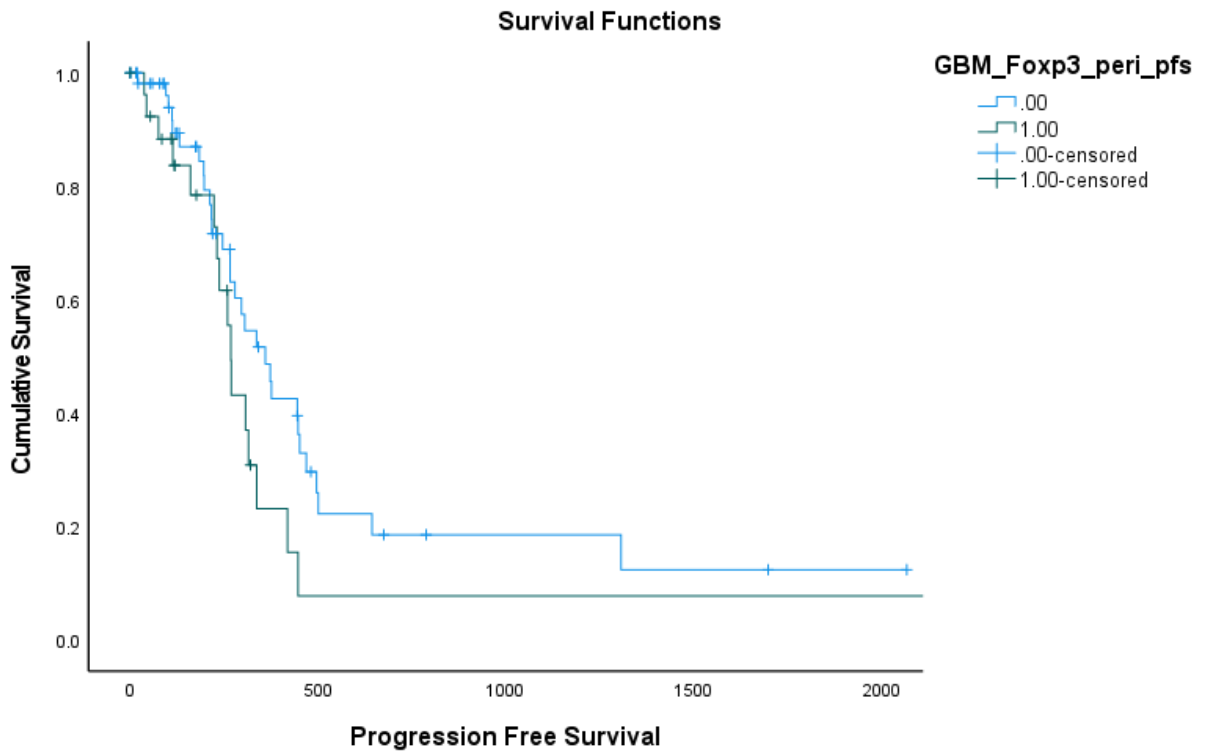


Figure 27: Density of FoxP3+ cells (per mm<sup>2</sup>) in the periphery in relation to progression free survival in days from surgery (p= .122). Green line: group with higher cell density, blue line: group with lower cell density

Figure 27 shows the progression free survival of GBM patients having a high density of FoxP3+ Tregs compared to that of the patients with a low density of FoxP3+ Tregs in the peripheral zone of the tumor observed over a period of 2000 days. No significant differences were observed (p=0.122)

9. FoxP3+ cell density in normal tissue and overall survival

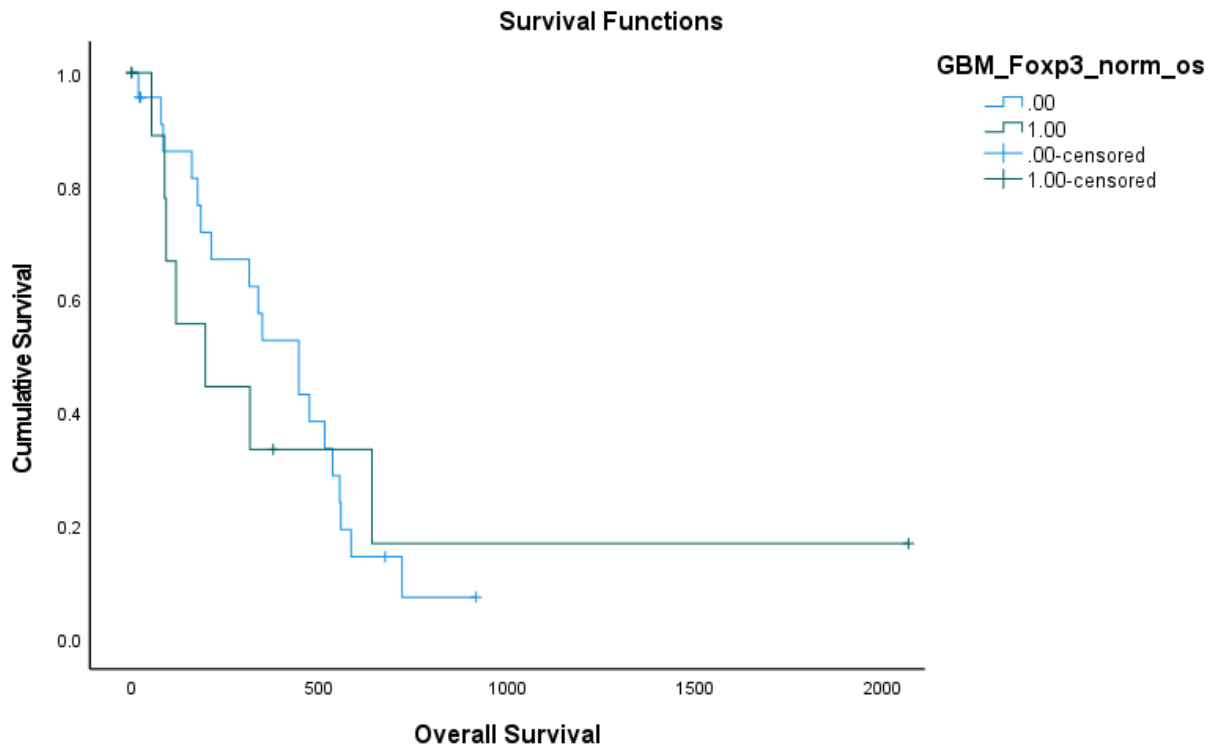


Figure 28: Density of FoxP3+ cells (per mm<sup>2</sup>) in the normal tissue around tumor in relation to overall survival in days from surgery (p= .824). Green line: group with higher cell density, blue line: group with lower cell density

In this Kaplan-Meier plot (Figure 28) the overall survival of GBM patients having a high density of Tregs in the normal tissue adjacent to tumor is compared to that of the patients with a low density of these cells in the same region. No significant differences were noted (p=.824).

10. FoxP3+ cell density in normal tissue and progression free survival

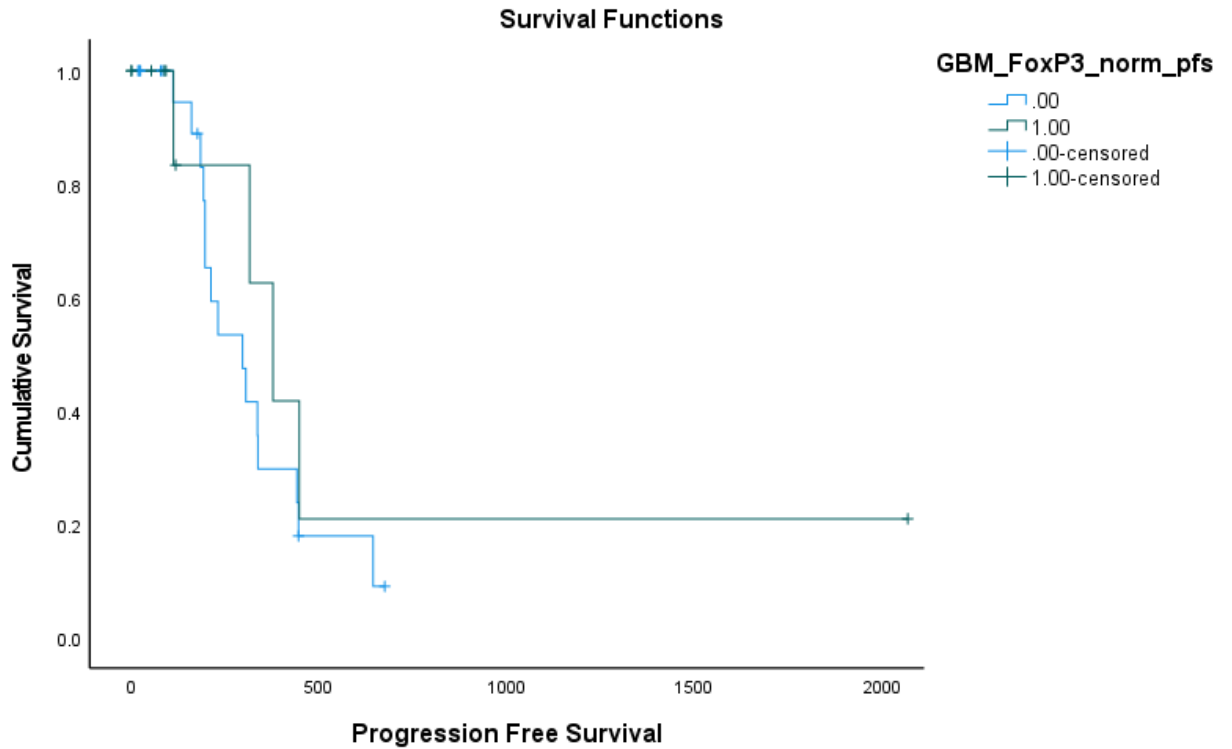


Figure 29: Density of FoxP3+ cells (per mm<sup>2</sup>) in the normal tissue around tumor in relation to progression free survival in days from surgery (p= .408). Green line: group with higher cell density, blue line: group with lower cell density

Figure 29 depicts the variation in the progression free survival of patients having a high density of Tregs in the normal tissue adjacent to tumor compared to that of the patients with a low density of these cells in the same region. No significant differences were noted (p=.408).

## **7 Discussion**

### **7.1 Method**

A double staining method that exploited the specific proteins namely the CD8 and the FoxP3 expressed in the cytotoxic T cells and regulatory T cells respectively were used to stain these cells in the tissue samples. With the help of computer programs, these immune cells were quantified and analyzed in self-specified 5 ROI: tumor core, necrotic zone, infiltration zone, peripheral zone and normal tissue surrounding the tumor.

Tissue microarrays initially called “multi-tumor (sausage) tissue blocks,” are a convenient method employed as an alternative for conventional tissue sections. It is increasingly used to study large sets of patient tissue. This process helps conserve precious tissue resources and reduces immunohistochemistry expenses (Battifora, 1986; Wen-Hui Wan, Fortuna, & Furmanski, 1987). We employed this method to process up to 81 tissue sections per array, which helped in saving a lot of time in the preparation and staining of the samples. There has been doubts initially that the small tissue area of the samples in this method might not represent the true tumor characteristics as the traditional whole sections does. But many validation studies for TMA on different tumors has shown its efficacy. For instance in breast cancer there is a similarity of 95% between the observations from one or two TMA cores and that from whole sections (Camp, Charette, & Rimm, 2000). Another study on ovarian cancer by Rosen et al. found out that analyzing two cores of a larger diameter of 1 mm is enough to get outcomes that coincide with conventional tissue sections. In our study we examined multiple cores for each ROI and the size of the cores examined were approximately 4 mm<sup>2</sup> each. This ensured an accurate representation of the tumor as whole sections would.

## **7.2 Results**

The impact of two important subgroups of TILs, namely the CD8<sup>+</sup> cytotoxic T-cells and the FoxP3<sup>+</sup> Tregs on the prognosis among GBM patients were studied. To attain a better understanding of their immune activity in the TME, at first they were quantified in the 5 ROI. As shown in Figures 7 - 9, it could be derived that the FoxP3<sup>+</sup> cells are found in much fewer numbers as compared to CD8<sup>+</sup> cells in each ROI. The density of CD8<sup>+</sup> cells didn't seem to vary significantly between tumor core, necrotic zone, infiltration zone and peripheral zone. The normal brain tissue adjacent to tumor showed significantly lesser number of CD8<sup>+</sup> cells compared to the other 4 ROI. The analysis of FoxP3<sup>+</sup> cell density also showed similar results. The mean cell density of both kinds of TILs decreased with increasing distance from the tumor core except in the infiltration zone which seemed to have a slightly higher density than necrotic zone (Figure 9). Virtually no FoxP3<sup>+</sup> cells could be detected in the adjacent normal brain tissue.

In the next step TIL density in each ROI was correlated with overall survival and progression free survival using Kaplan-Meier plots (Figure 10 - 29). The patients with a lower CD8<sup>+</sup> cell density at the tumor core was found to have a better overall survival ( $p=0.028$ ). Neither overall survival nor progression free survival seemed to be influenced by CD8<sup>+</sup> cell density in the other ROI. Nor could we find any significant correlation between FoxP3<sup>+</sup> cell density and survival.

## **7.3 TILs as prognostic factors in Glioblastoma**

### **7.3.1 CD8<sup>+</sup> cytotoxic T cells as a prognostic factor?**

Cytotoxic CD8<sup>+</sup> T cells constitute the backbone of anticancer immune response in most tumors and are the second most commonly occurring TILs in the TME of humans. As discussed earlier CD8<sup>+</sup> T lymphocytes infiltration is associated with better prognosis in many malignancies like ovarian cancer (Hwang, Adams, Tahirovic, Hagemann, & Coukos, 2012), HER-2 positive breast cancer (Salgado

et al., 2015), metastatic melanoma (Erdag et al., 2012), head and neck squamous cell carcinoma (Balermipas et al., 2016) etc.

When activated by the presentation of antigens bound on MHC 1 they kill neoplastic cells (Barnes & Amir, 2017). In our study we aimed at evaluating the prognostic significance of this very important group of immune cells in GBM.

With regard to GBM, the studies on the effect of CD8+ cell activity in TME have shown varying results. Some studies showed a prolonged survival in patients with higher CD8+ cell activity in TME (Kmiecik et al., 2013; Mauldin et al., 2021; Yang et al., 2010), were as Han et al. in 2014 and Sayour et al. in 2015 couldn't establish any positive correlation between the absolute number of CD8+ TILs and survival. Another study by Orrego et al. in 2018 higher levels CD8+ TILs in TME tend to predict shorter survival in GBM patients.

Although we could find considerable CD8+ cell activity in the TME of GBM, a conclusive correlation couldn't be established, except for the fact that a lower density of these cells at tumor core related to better overall survival. This coincides with the findings of Orrego et al. These inconsistent results suggests that immune activity that unfolds in the TME of GBM could be more complex than we know as of date. The findings of Sayour et al. that not the absolute numbers of TILs, but the increased ratio of CD3+ and CD8+ to FoxP3+ TILs were related to better survival and that of Han and his team that not CD8+ TIL activity alone but high ratio of CD4+ to that of CD8+ turned out to be a predictor of poor progress-free and overall survival further support this assumption.

More research is required to attain a finer understanding of the complex role CD8+ TILs play alone and together with other immune factors before a final statement can be made as to if CD8+ TILs or their ratio to other immune cells would deem as a reliable prognostic factor in GBM. This research could also pave the way for new immune therapy strategies capable of bringing about the much awaited breakthrough with regard to survival and quality of life in GBM.

### **7.3.2 FoxP3+ regulatory T cells as a prognostic factor?**

Tregs regulate the activity of T and B Lymphocytes, and play a vital role in maintaining homeostasis of CD8+ lymphocytes under physiological conditions. Deficits in Treg function leads to autoimmune diseases (Sakaguchi, Yamaguchi, Nomura, & Ono, 2008) and their deregulation leading to increased activity can be carcinogenic (Curiel et al., 2004). Tregs arising by tumor-driven conversion suppress anti-tumor immune responses and cancer-associated inflammation, which in turn favours tumor progression (Strauss et al., 2007; Whiteside, Schuler, & Schilling, 2012). They have a suppressive influence on CD8+ TILs which could lead to immune tolerance in cancers. Cytotoxic T-lymphocyte-associated Protein 4 (CTLA-4) expressed by activated Tregs suppress tumor-associated antigen presentation by APCs thus preventing the activation of cytotoxic T cells (Tanaka & Sakaguchi, 2017). In general increased Tregs in TME correlate with reduced overall survival as it has been demonstrated in many cancers like breast cancer, cervix cancer etc. (Shang et al., 2015). However a study on colorectal cancer by Salama et al., 2009 found out that high density of Tregs were associated with improved survival which is contradictory to the outcomes documented in other solid tumors.

Yue et al. (2014) found that regulatory FoxP3+ TILs negatively influence the progression-free and overall survival in GBM whereas a study by Thomas et al. in 2015 on a smaller patient population of 25 patients questioned this result. Our study further underlines this unpredictability of Treg activity in GBM as no correlation could be found between progression free or overall survival and Treg density in the different ROI. Although increased Treg activity seem to correlate with poor prognosis in most tumors studied till date, the studies on how their activity affects prognosis in GBM seem to yield discrepant conclusions. The mechanisms of Treg mediated immune regulation are not fully understood and should be further studied keenly, as the answers could hold the key to improving immune therapy exceptionally.



## 8 Bibliography

- Albert, F. K., Forsting, M., Sartor, K., Adams, H. P., & Kunze, S. (1994). Early postoperative magnetic resonance imaging after resection of malignant glioma: Objective evaluation of residual tumor and its influence on regrowth and prognosis. *Neurosurgery*, *34*(1). <https://doi.org/10.1097/00006123-199401000-00008>
- Álvaro, T., Lejeune, M., Salvadó, M. T., Bosch, R., García, J. F., Jaén, J., ... Piris, M. A. (2005). Outcome in Hodgkin's lymphoma can be predicted from the presence of accompanying cytotoxic and regulatory T cells. *Clinical Cancer Research*, *11*(4). <https://doi.org/10.1158/1078-0432.CCR-04-1869>
- Balermipas, P., Rödel, F., Rödel, C., Krause, M., Linge, A., Lohaus, F., ... Fokas, E. (2016). CD8+ tumour-infiltrating lymphocytes in relation to HPV status and clinical outcome in patients with head and neck cancer after postoperative chemoradiotherapy: A multicentre study of the German cancer consortium radiation oncology group (DKTK-ROG). *International Journal of Cancer*, *138*(1). <https://doi.org/10.1002/ijc.29683>
- Barnes, T. A., & Amir, E. (2017). HYPE or HOPE: The prognostic value of infiltrating immune cells in cancer. *British Journal of Cancer*, Vol. 117. <https://doi.org/10.1038/bjc.2017.220>
- Battifora, H. (1986). Methods in laboratory investigation. The multitumor (sausage) tissue block: Novel method for immunohistochemical antibody testing. *Laboratory Investigation*, *55*(2).
- Berghoff, A. S., Kiesel, B., Widhalm, G., Rajky, O., Ricken, G., Wohrer, A., ... Wick, W. (2015). Programmed death ligand 1 expression and tumor-infiltrating lymphocytes in glioblastoma. *Neuro-Oncology*, *17*(8). <https://doi.org/10.1093/neuonc/nou307>
- Bette, S., Gempt, J., Huber, T., Boeckh-Behrens, T., Ringel, F., Meyer, B., ... Kirschke, J. S. (2016). Patterns and Time Dependence of Unspecific Enhancement in Postoperative Magnetic Resonance Imaging after Glioblastoma Resection. *World Neurosurgery*, *90*. <https://doi.org/10.1016/j.wneu.2016.03.031>
- Bleeker, F. E., Molenaar, R. J., & Leenstra, S. (2012). Recent advances in the molecular understanding of glioblastoma. *Journal of Neuro-Oncology*. <https://doi.org/10.1007/s11060-011-0793-0>
- Camp, R. L., Charette, L. A., & Rimm, D. L. (2000). Validation of tissue microarray technology in breast carcinoma. *Laboratory Investigation*, *80*(12). <https://doi.org/10.1038/labinvest.3780204>

- Cloughesy, T. F., Petrecca, K., Walbert, T., Butowski, N., Salacz, M., Perry, J., ... Vogelbaum, M. A. (2020). Effect of Vocimagene Amiretrorepvec in Combination with Flucytosine vs Standard of Care on Survival following Tumor Resection in Patients with Recurrent High-Grade Glioma: A Randomized Clinical Trial. *JAMA Oncology*, 6(12).  
<https://doi.org/10.1001/jamaoncol.2020.3161>
- Coley WB. (1893). The treatment of malignant tumors by repeated inoculations of erysipelas. With a report of ten original cases. *Clin Orthop Relat Res*, Jan(262).
- Curiel, T. J., Coukos, G., Zou, L., Alvarez, X., Cheng, P., Mottram, P., ... Zou, W. (2004). Specific recruitment of regulatory T cells in ovarian carcinoma fosters immune privilege and predicts reduced survival. *Nature Medicine*, 10(9). <https://doi.org/10.1038/nm1093>
- Dandy, W. E. (1928). Removal of right cerebral hemisphere for certain tumors with hemiplegia: Preliminary report. *Journal of the American Medical Association*, 90(11). <https://doi.org/10.1001/jama.1928.02690380007003>
- Dolecek, T. A., Propp, J. M., Stroup, N. E., & Kruchko, C. (2012). CBTRUS statistical report: Primary brain and central nervous system tumors diagnosed in the United States in 2005-2009. *Neuro-Oncology*, Vol. 14.  
<https://doi.org/10.1093/neuonc/nos218>
- Domínguez-Soto, A., Sierra-Filardi, E., Puig-Kröger, A., Pérez-Maceda, B., Gómez-Aguado, F., Corcuera, M. T., ... Corbí, A. L. (2011). Dendritic Cell-Specific ICAM-3–Grabbing Nonintegrin Expression on M2-Polarized and Tumor-Associated Macrophages Is Macrophage-CSF Dependent and Enhanced by Tumor-Derived IL-6 and IL-10. *The Journal of Immunology*, 186(4). <https://doi.org/10.4049/jimmunol.1000475>
- Echarti, A., Hecht, M., Büttner-Herold, M., Haderlein, M., Hartmann, A., Fietkau, R., & Distel, L. (2019). Cd8+ and regulatory T cells differentiate tumor immune phenotypes and predict survival in locally advanced head and neck cancer. *Cancers*, 11(9). <https://doi.org/10.3390/cancers11091398>
- Erdag, G., Schaefer, J. T., Smolkin, M. E., Deacon, D. H., Shea, S. M., Dengel, L. T., ... Slingluff, C. L. (2012). Immunotype and immunohistologic characteristics of tumor-infiltrating immune cells are associated with clinical outcome in metastatic melanoma. *Cancer Research*, 72(5).  
<https://doi.org/10.1158/0008-5472.CAN-11-3218>
- Forsting, M., Albert, F. K., Kunze, S., Adams, H. P., Zenner, D., & Sartor, K. (1993). Extirpation of glioblastomas: MR and CT follow-up of residual tumor and regrowth patterns. *American Journal of Neuroradiology*, 14(1).
- González-Darder, J. M., González-López, P., Talamantes, F., Quilis, V., Cortés,

- V., García-March, G., & Roldán, P. (2010). Multimodal navigation in the functional microsurgical resection of intrinsic brain tumors located in eloquent motor areas: Role of tractography. *Neurosurgical Focus*, 28(2). <https://doi.org/10.3171/2009.11.FOCUS09234>
- Han, S., Zhang, C., Li, Q., Dong, J., Liu, Y., Huang, Y., ... Wu, A. (2014). Tumour-infiltrating CD4+ and CD8+ lymphocytes as predictors of clinical outcome in glioma. *British Journal of Cancer*. <https://doi.org/10.1038/bjc.2014.162>
- Hartmann, C., Hentschel, B., Simon, M., Westphal, M., Schackert, G., Tonn, J. C., ... Weller, M. (2013). Long-term survival in primary glioblastoma with versus without isocitrate dehydrogenase mutations. *Clinical Cancer Research*, 19(18). <https://doi.org/10.1158/1078-0432.CCR-13-0017>
- Hegi, M. E., Liu, L., Herman, J. G., Stupp, R., Wick, W., Weller, M., ... Gilbert, M. R. (2008). Correlation of O6-methylguanine methyltransferase (MGMT) promoter methylation with clinical outcomes in glioblastoma and clinical strategies to modulate MGMT activity. *Journal of Clinical Oncology*, Vol. 26. <https://doi.org/10.1200/JCO.2007.11.5964>
- Hwang, W. T., Adams, S. F., Tahirovic, E., Hagemann, I. S., & Coukos, G. (2012). Prognostic significance of tumor-infiltrating T cells in ovarian cancer: A meta-analysis. *Gynecologic Oncology*, 124(2). <https://doi.org/10.1016/j.ygyno.2011.09.039>
- Kirson, E. D., Gurvich, Z., Schneiderman, R., Dekel, E., Itzhaki, A., Wasserman, Y., ... Palti, Y. (2004). Disruption of Cancer Cell Replication by Alternating Electric Fields. *Cancer Research*, 64(9). <https://doi.org/10.1158/0008-5472.CAN-04-0083>
- Kmieciak, J., Poli, A., Brons, N. H. C., Waha, A., Eide, G. E., Enger, P. Ø., ... Chekenya, M. (2013). Elevated CD3+ and CD8+ tumor-infiltrating immune cells correlate with prolonged survival in glioblastoma patients despite integrated immunosuppressive mechanisms in the tumor microenvironment and at the systemic level. *Journal of Neuroimmunology*. <https://doi.org/10.1016/j.jneuroim.2013.08.013>
- Kreisl, T. N., Kim, L., Moore, K., Duic, P., Royce, C., Stroud, I., ... Fine, H. A. (2009). Phase II trial of single-agent bevacizumab followed by bevacizumab plus irinotecan at tumor progression in recurrent glioblastoma. *Journal of Clinical Oncology*, 27(5). <https://doi.org/10.1200/JCO.2008.16.3055>
- Kucerova, P., & Cervinkova, M. (2016). Spontaneous regression of tumour and the role of microbial infection - possibilities for cancer treatment. *Anti-Cancer Drugs*, Vol. 27. <https://doi.org/10.1097/CAD.0000000000000337>
- Lacroix, M., Abi-Said, D., Fourney, D. R., Gokaslan, Z. L., Shi, W., DeMonte, F.,

- ... Sawaya, R. (2001). A multivariate analysis of 416 patients with glioblastoma multiforme: Prognosis, extent of resection, and survival. *Journal of Neurosurgery*, 95(2). <https://doi.org/10.3171/jns.2001.95.2.0190>
- Lescher, S., Schniewindt, S., Jurcoane, A., Senft, C., & Hattingen, E. (2014). Time window for postoperative reactive enhancement after resection of brain tumors: Less than 72 hours. *Neurosurgical Focus*, 37(6). <https://doi.org/10.3171/2014.9.FOCUS14479>
- Li, L., Zhu, X., Qian, Y., Yuan, X., Ding, Y., Hu, D., ... Wu, Y. (2020). Chimeric Antigen Receptor T-Cell Therapy in Glioblastoma: Current and Future. *Frontiers in Immunology*, Vol. 11. <https://doi.org/10.3389/fimmu.2020.594271>
- Louis, D. N., Ohgaki, H., Wiestler, O. D., Cavenee, W. K., Burger, P. C., Jouvet, A., ... Kleihues, P. (2007). The 2007 WHO classification of tumours of the central nervous system. *Acta Neuropathologica*, Vol. 114. <https://doi.org/10.1007/s00401-007-0243-4>
- Mahoney, K. M., Freeman, G. J., & McDermott, D. F. (2015). The next immune-checkpoint inhibitors: Pd-1/pd-l1 blockade in melanoma. *Clinical Therapeutics*, Vol. 37. <https://doi.org/10.1016/j.clinthera.2015.02.018>
- Mahvash, M., Hugo, H. H., Maslehaty, H., Mehdorn, H. M., & Stark, A. M. (2011). Glioblastoma multiforme in children: Report of 13 cases and review of the literature. *Pediatric Neurology*, 45(3). <https://doi.org/10.1016/j.pediatrneurol.2011.05.004>
- Massagué, J. (2008). TGFβ in Cancer. *Cell*, Vol. 134. <https://doi.org/10.1016/j.cell.2008.07.001>
- Mauldin, I. S., Jo, J., Wages, N. A., Yogendran, L. V., Mahmutovic, A., Young, S. J., ... Fadul, C. E. (2021). Proliferating CD8+ T cell infiltrates are associated with improved survival in glioblastoma. *Cells*, 10(12). <https://doi.org/10.3390/cells10123378>
- Morales, A., Eidinger, D., & Bruce, A. W. (1976). Intracavitary Bacillus Calmette Guerin in the treatment of superficial bladder tumors. *Journal of Urology*, 116(2). [https://doi.org/10.1016/s0022-5347\(17\)58737-6](https://doi.org/10.1016/s0022-5347(17)58737-6)
- Nelson, S. J., & Cha, S. (2003). Imaging glioblastoma multiforme. *Cancer Journal*, 9(2). <https://doi.org/10.1097/00130404-200303000-00009>
- Oertel, J., von Buttlar, E., Schroeder, H. W. S., & Gaab, M. R. (2005). Prognosis of gliomas in the 1970s and today. *Neurosurgical Focus*, 18(4). <https://doi.org/10.3171/foc.2005.18.4.13>
- Ohgaki, H., & Kleihues, P. (2005). Population-based studies on incidence,

- survival rates, and genetic alterations in astrocytic and oligodendroglial gliomas. *Journal of Neuropathology and Experimental Neurology*, Vol. 64. <https://doi.org/10.1093/jnen/64.6.479>
- Ohgaki, H., & Kleihues, P. (2007). Genetic pathways to primary and secondary glioblastoma. *American Journal of Pathology*, Vol. 170. <https://doi.org/10.2353/ajpath.2007.070011>
- Ohgaki, H., & Kleihues, P. (2013). The definition of primary and secondary glioblastoma. *Clinical Cancer Research*, Vol. 19. <https://doi.org/10.1158/1078-0432.CCR-12-3002>
- Omuro, A. (2013). Glioblastoma and Other Malignant Gliomas. *JAMA*, 310(17). <https://doi.org/10.1001/jama.2013.280319>
- Orrego, E., Castaneda, C. A., Castillo, M., Bernabe, L. A., Casavilca, S., Chakravarti, A., ... Ojeda, L. (2018). Distribution of tumor-infiltrating immune cells in glioblastoma. *CNS Oncology*, 7(4). <https://doi.org/10.2217/cns-2017-0037>
- Ostrom, Q. T., Fahmideh, M. A., Cote, D. J., Muskens, I. S., Schraw, J. M., Scheurer, M. E., & Bondy, M. L. (2019). Risk factors for childhood and adult primary brain tumors. *Neuro-Oncology*, Vol. 21. <https://doi.org/10.1093/neuonc/noz123>
- Patel, S. J., Sanjana, N. E., Kishton, R. J., Eidizadeh, A., Vodnala, S. K., Cam, M., ... Restifo, N. P. (2017). Identification of essential genes for cancer immunotherapy. *Nature*, 548(7669). <https://doi.org/10.1038/nature23477>
- Pegg, A. E., Dolan, M. E., & Moschel, R. C. (1995). Structure, Function, and Inhibition of O6-Alkylguanine-DNA Alkyltransferase. *Progress in Nucleic Acid Research and Molecular Biology*, 51(C). [https://doi.org/10.1016/S0079-6603\(08\)60879-X](https://doi.org/10.1016/S0079-6603(08)60879-X)
- Ranger, A. M., Patel, Y. K., Chaudhary, N., & Anantha, R. V. (2014). Familial syndromes associated with intracranial tumours: A review. *Child's Nervous System*, Vol. 30. <https://doi.org/10.1007/s00381-013-2309-z>
- Reardon, D. A., Brandes, A. A., Omuro, A., Mulholland, P., Lim, M., Wick, A., ... Weller, M. (2020). Effect of Nivolumab vs Bevacizumab in Patients with Recurrent Glioblastoma: The CheckMate 143 Phase 3 Randomized Clinical Trial. *JAMA Oncology*, 6(7). <https://doi.org/10.1001/jamaoncol.2020.1024>
- Rini, B. I., Battle, D., Figlin, R. A., George, D. J., Hammers, H., Hutson, T., ... Atkins, M. B. (2019). The society for immunotherapy of cancer consensus statement on immunotherapy for the treatment of advanced renal cell carcinoma (RCC). *Journal for ImmunoTherapy of Cancer*, 7(1). <https://doi.org/10.1186/s40425-019-0813-8>

- Rosen, D. G., Huang, X., Deavers, M. T., Malpica, A., Silva, E. G., & Liu, J. (2004). Validation of tissue microarray technology in ovarian carcinoma. *Modern Pathology*, 17(7). <https://doi.org/10.1038/modpathol.3800120>
- Roux, A., Roca, P., Edjlali, M., Sato, K., Zanello, M., Dezamis, E., ... Pallud, J. (2019). MRI atlas of IDH wild-type supratentorial glioblastoma: Probabilistic maps of phenotype, management, and outcomes. *Radiology*, 293(3). <https://doi.org/10.1148/radiol.2019190491>
- Salama, P., Phillips, M., Grieu, F., Morris, M., Zeps, N., Joseph, D., ... Iacopetta, B. (2009). Tumor-infiltrating FOXP3+ T regulatory cells show strong prognostic significance in colorectal cancer. *Journal of Clinical Oncology*, 27(2). <https://doi.org/10.1200/JCO.2008.18.7229>
- Salgado, R., Denkert, C., Demaria, S., Sirtaine, N., Klauschen, F., Pruneri, G., ... Loi, S. (2015). The evaluation of tumor-infiltrating lymphocytes (TILS) in breast cancer: Recommendations by an International TILS Working Group 2014. *Annals of Oncology*, Vol. 26. <https://doi.org/10.1093/annonc/mdu450>
- Santoemma, P. P., & Powell, D. J. (2015). Tumor infiltrating lymphocytes in ovarian cancer. *Cancer Biology and Therapy*, Vol. 16. <https://doi.org/10.1080/15384047.2015.1040960>
- Sayour, E. J., McLendon, P., McLendon, R., De Leon, G., Reynolds, R., Kresak, J., ... Mitchell, D. a. (2015). Increased proportion of FoxP3+ regulatory T cells in tumor infiltrating lymphocytes is associated with tumor recurrence and reduced survival in patients with glioblastoma. *Cancer Immunology, Immunotherapy : CII*, 64(4), 419–427. <https://doi.org/10.1007/s00262-014-1651-7>
- Schmidt, N. O., Westphal, M., Hagel, C., Ergün, S., Stavrou, D., Rosen, E. M., & Lamszus, K. (1999). Levels of vascular endothelial growth factor, hepatocyte growth factor/scatter factor and basic fibroblast growth factor in human gliomas and their relation to angiogenesis. *International Journal of Cancer*, 84(1). [https://doi.org/10.1002/\(SICI\)1097-0215\(19990219\)84:1<10::AID-IJC3>3.0.CO;2-L](https://doi.org/10.1002/(SICI)1097-0215(19990219)84:1<10::AID-IJC3>3.0.CO;2-L)
- Senga, S. S., & Grose, R. P. (2021). Hallmarks of cancer—the new testament. *Open Biology*, Vol. 11. <https://doi.org/10.1098/rsob.200358>
- Sevenich, L. (2019). Turning “Cold” into “Hot” tumors - Opportunities and challenges for radio-immunotherapy against primary and metastatic brain cancers. *Frontiers in Oncology*, Vol. 9. <https://doi.org/10.3389/fonc.2019.00163>
- Shang, B., Liu, Y., Jiang, S. J., & Liu, Y. (2015). Prognostic value of tumor-infiltrating FoxP3+ regulatory T cells in cancers: A systematic review and meta-analysis. *Scientific Reports*, 5. <https://doi.org/10.1038/srep15179>

- Speiser, D. E., Ho, P. C., & Verdeil, G. (2016). Regulatory circuits of T cell function in cancer. *Nature Reviews Immunology*, Vol. 16. <https://doi.org/10.1038/nri.2016.80>
- Strauss, L., Bergmann, C., Szczepanski, M., Gooding, W., Johnson, J. T., & Whiteside, T. L. (2007). A unique subset of CD4+CD25highFoxp3+ T cells secreting interleukin-10 and transforming growth factor- $\beta$ 1 mediates suppression in the tumor microenvironment. *Clinical Cancer Research*, 13(15). <https://doi.org/10.1158/1078-0432.CCR-07-0472>
- Stummer, W., Reulen, H. J., Meinel, T., Pichlmeier, U., Schumacher, W., Tonn, J. C., ... Stummer, W. (2008). Extent of resection and survival in glioblastoma multiforme: Identification of and adjustment for bias. *Neurosurgery*, 62(3). <https://doi.org/10.1227/01.neu.0000317304.31579.17>
- Stupp, R., Brada, M., van den Bent, M. J., Tonn, J. C., & Pentheroudakis, G. (2014). High-grade glioma: ESMO clinical practice guidelines for diagnosis, treatment and follow-up. *Annals of Oncology*, 25. <https://doi.org/10.1093/annonc/mdu050>
- Stupp, Roger, Mason, W., van den Bent, M. J., Weller, M., Fisher, B. M., Taphoorn, M. J. B., ... Mirimanoff, R. O. (2005). Radiotherapy plus Concomitant and Adjuvant Temozolomide for Glioblastoma. *The New England Journal of Medicine*, 987–996. <https://doi.org/10.1056/NEJMoa043330>
- Stupp, Roger, Taillibert, S., Kanner, A., Read, W., Steinberg, D. M., Lhermitte, B., ... Ram, Z. (2017). Effect of tumor-treating fields plus maintenance temozolomide vs maintenance temozolomide alone on survival in patients with glioblastoma a randomized clinical trial. *JAMA - Journal of the American Medical Association*, 318(23). <https://doi.org/10.1001/jama.2017.18718>
- Tanaka, A., & Sakaguchi, S. (2017). Regulatory T cells in cancer immunotherapy. *Cell Research*, Vol. 27. <https://doi.org/10.1038/cr.2016.151>
- Thomas, A. A., Fisher, J. L., Rahme, G. J., Hampton, T. H., Baron, U., Olek, S., ... Fadul, C. E. (2015). Regulatory T cells are not a strong predictor of survival for patients with glioblastoma. *Neuro-Oncology*. <https://doi.org/10.1093/neuonc/nou363>
- Tolnay, M. (2002). Neuropathologie glialer Hirntumoren. *Swiss Medical Forum – Schweizerisches Medizin-Forum*. <https://doi.org/10.4414/smf.2002.04595>
- Toms, S. A., Kim, C. Y., Nicholas, G., & Ram, Z. (2019). Increased compliance with tumor treating fields therapy is prognostic for improved survival in the treatment of glioblastoma: a subgroup analysis of the EF-14 phase III trial. *Journal of Neuro-Oncology*, 141(2). <https://doi.org/10.1007/s11060-018->

- Upadhyay, N., & Waldman, A. D. (2011). Conventional MRI evaluation of gliomas. *British Journal of Radiology*, 84(SPEC. ISSUE 2). <https://doi.org/10.1259/bjr/65711810>
- Vredenburgh, J. J., Cloughesy, T., Samant, M., Prados, M., Wen, P. Y., Mikkelsen, T., ... Friedman, H. S. (2010). Corticosteroid Use in Patients with Glioblastoma at First or Second Relapse Treated with Bevacizumab in the BRAIN Study. *The Oncologist*, 15(12). <https://doi.org/10.1634/theoncologist.2010-0105>
- Waldman, A. D., Fritz, J. M., & Lenardo, M. J. (2020). A guide to cancer immunotherapy: from T cell basic science to clinical practice. *Nature Reviews Immunology*, Vol. 20. <https://doi.org/10.1038/s41577-020-0306-5>
- Wang, S., Song, C., Zha, Y., & Li, L. (2016). The prognostic value of MGMT promoter status by pyrosequencing assay for glioblastoma patients' survival: A meta-analysis. *World Journal of Surgical Oncology*, Vol. 14. <https://doi.org/10.1186/s12957-016-1012-4>
- Wellenstein, M. D., & de Visser, K. E. (2018). Cancer-Cell-Intrinsic Mechanisms Shaping the Tumor Immune Landscape. *Immunity*, Vol. 48. <https://doi.org/10.1016/j.immuni.2018.03.004>
- Weller, M., Butowski, N., Tran, D. D., Recht, L. D., Lim, M., Hirte, H., ... Nag, S. (2017). Rindopepimut with temozolomide for patients with newly diagnosed, EGFRvIII-expressing glioblastoma (ACT IV): a randomised, double-blind, international phase 3 trial. *The Lancet Oncology*, 18(10). [https://doi.org/10.1016/S1470-2045\(17\)30517-X](https://doi.org/10.1016/S1470-2045(17)30517-X)
- Wen-Hui Wan, Fortuna, M. B., & Furmanski, P. (1987). A rapid and efficient method for testing immunohistochemical reactivity of monoclonal antibodies against multiple tissue samples simultaneously. *Journal of Immunological Methods*, 103(1). [https://doi.org/10.1016/0022-1759\(87\)90249-3](https://doi.org/10.1016/0022-1759(87)90249-3)
- Whiteside, T. L., Schuler, P., & Schilling, B. (2012). Induced and natural regulatory T cells in human cancer. *Expert Opinion on Biological Therapy*, Vol. 12. <https://doi.org/10.1517/14712598.2012.707184>
- Wöhrer, A., Waldhör, T., Heinzl, H., Hackl, M., Feichtinger, J., Gruber-Mösenbacher, U., ... Hainfellner, J. A. (2009). The Austrian Brain Tumour Registry: A cooperative way to establish a population-based brain tumour registry. *Journal of Neuro-Oncology*, 95(3). <https://doi.org/10.1007/s11060-009-9938-9>
- Yan, H., Parsons, D. W., Jin, G., McLendon, R., Rasheed, B. A., Yuan, W., ... Bigner, D. D. (2009). IDH1 and IDH2 Mutations in Gliomas. *New England*



*Journal of Medicine*, 360(8), 765–773.  
<https://doi.org/10.1056/nejmoa0808710>

Yang, I., Tihan, T., Han, S. J., Wrensch, M. R., Wiencke, J., Sughrue, M. E., & Parsa, A. T. (2010). CD8+ T-cell infiltrate in newly diagnosed glioblastoma is associated with long-term survival. *Journal of Clinical Neuroscience : Official Journal of the Neurosurgical Society of Australasia*, 17(11), 1381–1385. <https://doi.org/10.1016/j.jocn.2010.03.031>

Yue, Q., Zhang, X., Ye, H., Wang, Y., Du, Z., Yao, Y., & Mao, Y. (2014). The prognostic value of Foxp3+ tumor-infiltrating lymphocytes in patients with glioblastoma. *Journal of Neuro-Oncology*, 116(2), 251–259. <https://doi.org/10.1007/s11060-013-1314-0>

## 9 Abbreviations

APC	-	Antigen presenting cell
BBB	-	Blood Brain Barrier
BCG	-	Bacillus Calmette-Guérin
B Lymphocytes	-	Bone marrow derived Lymphocytes
CAR-T cells	-	Chimeric antigen receptor T cells
CD	-	Cluster of differentiation
CT	-	Computed Tomography
CTLA-4	-	cytotoxic T-lymphocyte-associated Protein 4
DNA	-	Deoxyribonucleic acid
EGFRvIII	-	Epidermal growth factor receptor variant III
FoxP3	-	Forkhead Box Protein P3
GBM	-	Glioblastoma
Gy	-	Gray
HE	-	Hematoxylin Eosin
IDH	-	Isocitrate dehydrogenase
IFN- $\gamma$	-	Interferon- $\gamma$
IL-10	-	Interleukin 10
KPS	-	Karnofsky performance score
MGMT	-	O6-Methylguanin-DNA-Methyltransferase
MHC	-	Major histocompatibility complex
MRI	-	Magnetic Resonance Imaging
RCT	-	Radiochemotherapy
ROI	-	Region of Interest
TAM	-	Tumor associated Macrophage
TGF- $\beta$	-	Transforming growth factor $\beta$
TIL	-	Tumor infiltrating Lymphocyte
T Lymphocytes	-	Thymus derived Lymphocytes
TMA	-	Tissue Microarrays
TME	-	Tumor Microenvironment

TMZ	-	Temozolomide
TNF	-	Tumor necrosis factor
Tregs	-	Regulatory T Lymphocytes
TRIS	-	Tris (hydroxymethyl) aminomethane
TTFields	-	Tumor treating fields
TWEEN	-	Polysorbate 20
VEGF	-	Vascular Endothelial Growth Factor
WHO	-	World Health Organization

## 10 Illustrations

- Figure 1: Histopathology of Glioblastoma showing pseudopalisading(1) with necrosis(2) of neoplastic cells along with microvascular proliferation(3) (source: [webpath.med.utah.edu](http://webpath.med.utah.edu), accessed on 01.06.2022)..... 13
- Figure 2: Different MRI modalities of a female patient aged 55 with multifocal GBM - T1 weighted (A), T1-weighted enhanced with Gadolinium (B), T2 weighted (C), FLAIR (D). (Department of Neurosurgery, Klinikum Deggendorf) ..... 15
- Figure 3: preoperative (A) and postoperative (B) axial Gadolinium-enhanced T1-weighted MR images of a 60 year old male (Department of Neurosurgery, Klinikum Deggendorf) ..... 17
- Figure 4: Stupp Regimen (Gilbert and Armstrong 2007) ..... 18
- Figure 5: Hallmarks of cancer (Hanahan and Weinberg 2011)..... 22
- Figure 6: Schematic presentation of the tissue microarray method. (Nilbert and Engellau, 2004)..... 26
- Figure 7: Box plot depicting the cell density in cells/mm<sup>2</sup> of CD8+ TILs. The median cell density seems to drop from the tumor core towards the normal tissue except for an increase in the infiltration zone. .... 30
- Figure 8: Box plot depicting the cell density in cells/mm<sup>2</sup> of FoxP3+ TILs. The median cell density seems to drop from the tumor core towards the normal tissue except for a slight increase in the infiltration zone. .... 31
- Figure 9: Here the mean cell densities of the CD8+ TILs are compared with FoxP3+ TILs in the different ROI. .... 32
- Figure 10: Density of CD8+ cells per mm<sup>2</sup> at tumor core in relation to overall survival in days after surgery (p=.028). Green line: group with higher cell density than median, blue line: group with lower cell density than median. .... 33
- Figure 11: Density of CD8+ cells (per mm<sup>2</sup>) at tumor core in relation to progression free survival in days from surgery (p= .471). Green line: group with higher cell density, blue line: group with lower cell density ..... 34
- Figure 12: Density of CD8+ cells (per mm<sup>2</sup>) in tumor necrosis in relation to overall survival in days (p= .364). Green line: group with higher cell density, blue line: group with lower cell density. .... 35

Figure 13: Density of CD8+ cells (per mm<sup>2</sup>) in tumor necrosis in relation to progression free survival in days (p= .350). Green line: group with higher cell density, blue line: group with lower cell density ..... 36

Figure 14: Density of CD8+ cells (per mm<sup>2</sup>) in infiltration zone in relation to overall survival in days (p= .492). Green line: group with higher cell density, blue line: group with lower cell density ..... 37

Figure 15: Density of CD8+ cells (per mm<sup>2</sup>) in infiltration zone in relation to progression free survival in days (p=.617). Green line: group with higher cell density, blue line: group with lower cell density ..... 38

Figure 16: Density of CD8+ cells (per mm<sup>2</sup>) in peripheral zone in relation to overall survival in days (p=.191). Green line: group with higher cell density, blue line: group with lower cell density ..... 39

Figure 17: Density of CD8+ cells (per mm<sup>2</sup>) in peripheral zone in relation to progression free survival in days (p= .294). Green line: group with higher cell density, blue line: group with lower cell density ..... 40

Figure 18: Density of CD8+ cells (per mm<sup>2</sup>) in normal tissue in relation to overall survival in days (p= .659). Green line: group with higher cell density, blue line: group with lower cell density ..... 41

Figure 19: Density of CD8+ cells (per mm<sup>2</sup>) in normal tissue in relation to progression free survival after surgery in days (p= .523). Green line: group with higher cell density, blue line: group with lower cell density ..... 42

Figure 20: Density of FoxP3+ cells (per mm<sup>2</sup>) in tumor core in relation to overall survival in days from surgery (p= .501). Green line: group with higher cell density, blue line: group with lower cell density ..... 43

Figure 21: Density of FoxP3+ cells (per mm<sup>2</sup>) in tumor core in relation to progression free survival in days from surgery (p= .594). Green line: group with higher cell density, blue line: group with lower cell density ..... 44

Figure 22: Density of FoxP3+ cells (per mm<sup>2</sup>) in tumor necrosis in relation to overall survival in days from surgery (p= .370). Green line: group with higher cell density, blue line: group with lower cell density ..... 45

Figure 23: Density of FoxP3+ cells (per mm<sup>2</sup>) in tumor necrosis in relation to progression free survival in days from surgery (p= .807). Green line: group with higher cell density, blue line: group with lower cell density ..... 46

Figure 24: Density of FoxP3+ cells (per mm<sup>2</sup>) in the infiltration zone relation to overall survival in days from surgery (p= .360). Green line: group with higher cell density, blue line: group with lower cell density ..... 47

Figure 25: Density of FoxP3+ cells (per mm<sup>2</sup>) in the infiltration zone relation to progression free survival in days from surgery (p= .522). Green line: group with higher cell density, blue line: group with lower cell density ..... 48

Figure 26: Density of FoxP3+ cells (per mm<sup>2</sup>) in the periphery in relation to overall survival in days from surgery (p= .054). Green line: group with higher cell density, blue line: group with lower cell density..... 49

Figure 27: Density of FoxP3+ cells (per mm<sup>2</sup>) in the periphery in relation to progression free survival in days from surgery (p= .122). Green line: group with higher cell density, blue line: group with lower cell density ..... 50

Figure 28: Density of FoxP3+ cells (per mm<sup>2</sup>) in the normal tissue around tumor in relation to overall survival in days from surgery (p= .824). Green line: group with higher cell density, blue line: group with lower cell density ..... 51

Figure 29: Density of FoxP3+ cells (per mm<sup>2</sup>) in the normal tissue around tumor in relation to progression free survival in days from surgery (p= .408). Green line: group with higher cell density, blue line: group with lower cell density ..... 52

## **11 Acknowledgement**

I heartily thank Prof. Dr. med. Rainer Fietkau for making my doctoral thesis possible under his supervision at the Radiation Clinic.

I am very grateful to Prof. Dr. Distel who readily and patiently assisted and guided me throughout this project. All his knowledge and tips made my work enjoyable and easier.

Furthermore, I thank Dr. Bloß and Prof. Dr. Grabenbauer who helped me find this project. Dr. Bloß actively supported me and helped me collect all the data and slides for the research. I would also like to thank PD Dr. Monoranu for providing me all the necessary know how required to work with the histological specimen.

PD Dr. Carolus and PD Dr. Brenke are two other important persons i am very thankful to and whose help and support i would like to remember on this occasion.

Last but not the least I am grateful to my parents who have always been there for me.